(19) Europäisches Patentamt
European Patent Office
Office européen des brevets

(11) **EP 4 559 577 A1**

(12) **EUROPEAN PATENT APPLICATION**

(43) Date of publication:
**28.05.2025 Bulletin 2025/22**

(21) Application number: **23461682.9**

(22) Date of filing: **24.11.2023**

(51) International Patent Classification (IPC):
***B01L 3/00*** *(2006.01)* ***B01L 3/02*** *(2006.01)*

(52) Cooperative Patent Classification (CPC):
**B01L 3/0251; B01L 3/502784; B01L 3/5088;**
B01L 2200/027; B01L 2200/0673; B01L 2300/0816; B01L 2300/0838; B01L 2300/0867; B01L 2300/161; B01L 2400/0478; B01L 2400/0487

(84) Designated Contracting States:
**AL AT BE BG CH CY CZ DE DK EE ES FI FR GB GR HR HU IE IS IT LI LT LU LV MC ME MK MT NL NO PL PT RO RS SE SI SK SM TR**
Designated Extension States:
**BA**
Designated Validation States:
**KH MA MD TN**

(71) Applicant: **Instytut Chemii Fizycznej Polskiej Akademii Nauk**
**01-224 Warszawa (PL)**

(72) Inventors:
- **Navarette, Jonathan Pullas**
  **01-175 Warszawa (PL)**
- **Guzowski, Jan**
  **02-717 Warszawa (PL)**
- **Mallea, Ronald Terrazas**
  **01-231 Warszawa (PL)**

(74) Representative: **Witek, Rafal**
**WTS Patent Attorneys**
**Witek, Sniezko & Partners**
**Ul. Rudolfa Weigla 12**
**53-114 Wroclaw (PL)**

(54) **A DEVICE, METHOD AND A USE OF THE DEVICE FOR PRINTING ORDERED ARRAYS OF DOUBLE-EMULSION DROPLETS AT A SUBSTRATE UNDER AN EXTERNAL AQUEOUS PHASE**

(57) First object of the invention is a device for printing ordered arrays of double-emulsion droplets at a substrate under an external aqueous phase comprising a movable printing system comprising a movable stage in Y direction and an application system, and the application system comprises an actuator movable in X-Z directions to which a print head is attached wherein the print head is fluidly connected to the source of a dispersed phase and at least one source of dispersing phase, where the printhead comprises a dispersed phase inlet, at least one dispersant phase inlet, and the inlets are fluidly connected to an outlet channel connected to a chamber for attaching an application needle, characterised in that the chamber for attaching the application needle is parallel and coaxial or perpendicular to the outlet channel, wherein inner surface of the needle is rendered hydrophobic, preferably fluorophilic, wherein outer surface of the needle is susceptible to wetting by the external phase, and the movable stage comprises a substrate with a modified surface for dispensing a train of monodisperse carrier particles. Another object of the invention is a method of printing ordered arrays of double-emulsion droplets on a substrate under an external phase. Further object of the invention is use of the device for printing ordered arrays of double-emulsion droplets at a substrate under an external aqueous phase.

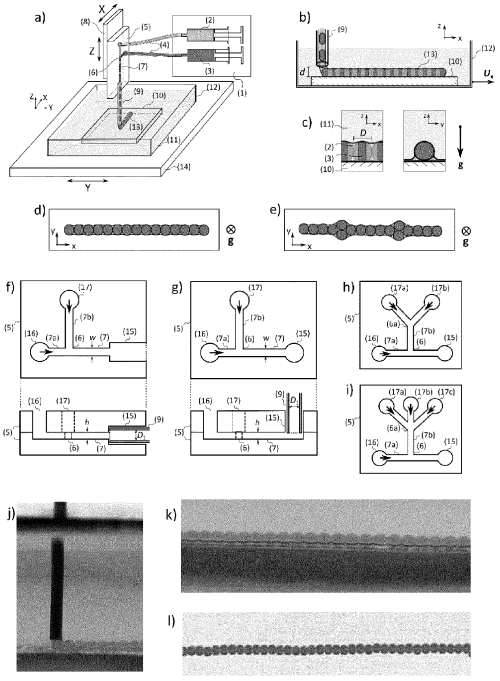

Figure 1

EP 4 559 577 A1

## Description

### Summary

**[0001]** The invention relates to a device for direct writing (printing) of monodisperse double emulsion droplets, e.g., W/O/W (water-in-oil-in-water), such that the inner droplets are extruded one-by-one onto a substrate in a form of a chain, a double chain, or an intermediate linear structure, while being immersed within an external aqueous environment, as well as to the method of the long-term stabilization of the printed droplet structures through the use of a substrate with modified topography and surface chemistry and to the method of such substrate modification. The invention finds applications in cell encapsulation for high-throughput screening of drugs, biomaterials, or other active substances that require culturing of cells inside the droplets under an external aqueous environment. In particular, the method allows for the identification of the droplets via their sequential deposition and efficient immobilization at the substrate in the form of a chain or a perturbed chain.

### Background of the invention

**[0002]** Droplet microfluidics, a set of techniques aimed at the generation and manipulation of microscopic (submillimeter) droplets in microchannels, has been attracting increasing attention in biotechnology, biomedicine, and materials science as a route towards miniaturization of biological and/or biochemical assays [1-3] and the development of new soft materials [4, 5].

**[0003]** Droplet microfluidics relies on the generation of droplets of one liquid phase inside the other external immiscible liquid phase, i.e., the formation of an emulsion, such as oil-in-water (O/W) or water-in-oil (W/O) emulsions. More complex so-called double emulsions, in which each droplet engulfs smaller droplets of another liquid phase, can also be formed. Of particular interest are water-in-oil-in-water (W/O/W) double emulsions, i.e., liquid core-shell architectures, in which oil 'shells' suspended in an external aqueous phase encapsulate smaller aqueous 'cores'. These kinds of systems have been reported to be suitable, e.g., for encapsulation of living cells inside the aqueous cores [6]-[11].

**[0004]** Conventional methods of generation of double-emulsions, such as (i) two-step emulsification in which the inner and the external aqueous phases are prepared separately and emulsified using high-speed homogenizers, or (ii) phase inversion techniques, are widely used but often yield double-emulsions of low stability and, typically, low monodispersity. Accordingly, the droplets are subject to the Ostwald ripening upon storage or when exposed to environmental stresses [12]. Finally, and perhaps most importantly, the droplets in such emulsions are difficult to be addressed individually (monitored, manipulated, etc.), which poses a problem, e.g., in high-throughput screening applications.

**[0005]** In comparison, microfluidic platforms are very effective in terms of massive production of highly monodisperse double-emulsion droplets comprising of single or multiple cores [7], [13]. The microfluidic double-emulsion droplet generators typically exploit two (or more) nested junctions, including concentric capillaries, cross-flow, co-flow, flow-focusing, or T-junctions [14]-[16]. It has been demonstrated that, via adjusting the rates of flow of the three liquid phases (external-, shell- and core phase), it is possible to control the sizes of the core and the shell as well as the number of cores in each shell [17], [18].

**[0006]** In terms of the screening applications, monodisperse double-emulsions can be processed in reproducible manner using e.g., flow cytometry [19]. In fact, at sufficiently low droplet volumes, monodispersity of the droplets warrants that no more than a single cell is encapsulated in each droplet. Such approach opens way to the high-throughput single-cell analyses, e.g., using FACS [20].

**[0007]** Double-emulsions have also been employed as encapsulants for multiple cells (tens to hundreds) for the purpose of controlled cell aggregation and formation of the so-called cell spheroids or microtissues. In this respect, microfluidics offers excellent control and allows fabrication of microtissues of monodisperse sizes and/or well-defined cellular composition [21], [22]. The cells aggregate within several hours after droplet generation, and they can be extracted from the droplets without compromising the integrity of thus formed spheroids [21]. In particular, the close-packed 3D spatial arrangement of cells within the spheroid mimics the arrangement of cells in an actual tissue. Accordingly, the spheroids have been widely used as microscopic 'tissue probes' for high-throughput testing of drugs including toxicity or efficacy (e.g., liver spheroids [23] or tumor spheroids [8]) or as granular building blocks for fabrication of larger tissue-like constructs [21]. Generation of spheroids using microfluidic double-emulsions provides, besides superior monodispersity, also high throughput and practically unlimited capacity. In fact, microfluidic devices can generate the droplets in a continuous manner such that the total number of the generated spheroids is limited only by the time of operation of the device or the volume of the to-be-dispersed cell suspension.

**[0008]** The double-emulsion approach facilitates recovery of the cells or cell spheroids from the inner aqueous droplets and their rapid transfer to the external aqueous phase (the culture medium) via braking of the oil shells [11], [22]. Even when encapsulated inside the inner aqueous cores, the cells can be cultured at high viability for at least 48 h [11]. Viability of cells at longer times (>2 days) has not been much investigated, however, it is known that some types of surfactants (in the oil

phase) promote transport of large biomolecules or even nanoparticles through the oil shells [24] which suggests possibility of the delivery of nutrients to the inner aqueous cores from the external medium at long culture times.

**[0009]** Although the generation of double-emulsion microdroplets using microfluidics has been already well established, additional droplet operations, including labelling, sorting, and precision-dispensing, are a subject of ongoing research and rapid technological advancements. In particular, droplet labelling, also referred to as 'barcoding', which allows to identify each of the thousands of monodisperse droplets poses a significant challenge and often remains a bottleneck in the screening applications [25]. The currently available methods of droplet labelling include: (i) injection of a dye (or dye combinations) at different concentrations inside the droplets [26], [27], (ii) direct enumeration and 1D-ordering of the droplets inside a narrow tubing [28], [29], (iii) 1D-ordering in a tubing and barcoding via generation of additional 'passive' droplets [30], (iv) 2D-trapping of the droplets on-chip using an array of prefabricated geometric traps [27], and (v) precision-dispensing of droplets one-by-one into prefabricated traps at a substrate via using dielectrophoresis [31], preferential wetting [32], [33], or via steric forces [34].

**[0010]** The available microfluidic labelling methods typically suffer from either low capacity (small number of available labels/barcodes) or high-complexity of generation/readout system. Tomasi et al. demonstrated a platform for trapping and incubation of droplets containing cell-spheroids which could be cultured for up to 3 days [27] or-after droplet gelation and replacement of oil with a culture medium-even up to 7 days [35]. The droplets were labelled using dye combinations [27] or could be identified based on their position in the array [35]. In the case of the dyed droplets, the barcoding capacity was limited to only $N = 3^3 = 27$ dye combinations, which was quite modest in view of the actual demands in typical high-throughput screening applications. Cole et al. [31] deposited $N = 100 \times 100 = 10^4$ individually addressable droplets into a square array at a substrate thus elevating the screening capacity by nearly 3 orders of magnitude. Importantly, in this case, the open-top configuration of the platform allowed injection or aspiration from individual droplets on-demand using a microcapillary mounted on an automated XYZ-stage. However, the functionality of the system was demonstrated only at relatively short-term culture times (several hours). The platform was also quite complex as it required prefabrication of $N = 10^4$ dielectric traps at the substrate. Other types of microfabricated traps have also been reported [32], [36]. In all these cases, the preparation of precisely structured substrates elevates the complexity and/or cost of the droplet labelling method.

**[0011]** In contrast, no special substrate was required in the method proposed recently by Li et al. [37] who used a photosensitive resin as the continuous phase to co-extrude the aqueous droplets onto a flat, smooth substrate. The resin was immediately solidified upon extrusion by UV light which allowed printing of stable linear arrays of equally spaced droplets embedded in the resin which could be identify based on their sequential deposition. However, cell culture under the resin has not been demonstrated. In fact, it would most likely lead to issues associated with resin cytotoxicity and its low permeability to gases.

**[0012]** In another approach, Nelson et al. [38] printed arrays of aqueous droplets under an external PDMS oil-based yield-stress fluid bath. The authors demonstrated the use of the platform in antibiotic susceptibility testing via co-encapsulating bacteria and antibiotics inside the droplets. Despite simplicity of the approach, the throughput of the method was limited by relatively low frequency of droplet generation (~1 Hz) and large spacing between the droplets (over 1 mm).

**[0013]** Hydrogel droplet chains, consisting of elongated droplets (plugs) labelled by different dyes, were fabricated by Ma [39] using direct extrusion from a PTFE (polytetrafluoroethylene) tubing under an external oil phase. No application of the method in high-throughput droplet barcoding has been demonstrated but one can expect that the barcoding capacity in this case would be limited by the number of different dyes.

**[0014]** Finally, Zhou et al. [40] demonstrated printing of cell-laden aqueous droplets under external lipid-oil phase. The authors used piezo-actuators to generate cross linkable Matrigel droplets which subsequently sedimented freely onto a substrate. The stability of the assembled droplet-constructs relied on the droplet-droplet adhesion mediated by the formation of the droplet-interface lipid bilayers (DIBs). After gelation, the construct could be transferred into cell medium for culture [40]. Despite promising applications in 3D printing of complex organoids the method is not suitable for generation of ordered arrays of droplets (either 1D or 2D) unless these printed droplets are surrounded by a co-printed droplet-bath whose fabrication is extremely time consuming [41].

**[0015]** In the Polish patent application P.433162 [42] is disclosed a method of labelling monodisperse carrier particles comprising the steps of: creating carrier particles in suspension, applying carrier particles to a substrate, imaging, whereby the imaging step includes: identifying a selected single carrier particle and/or identifying all carrier particles sequentially; wherein the stage of generating carrier particles, a suspension of carrier particles containing each a mixture of cells and/or chemicals is generated, with the cells and/or chemicals being fed to the carrier particles sequentially according to a defined protocol such that the next carrier particle generated contains a known mixture of cells and/or chemicals, and in the step of applying the carrier particles to the substrate, the carrier particles are applied to the substrate in the form of a chain, characterized in that the carrier particles containing cells and/or chemicals in suspension are applied from the application needle one by one to the surface of the substrate, whereby when the rate of feeding $f_{feed}$ of carrier particles from the application needle to the substrate is equal to the rate of transfer (advection) $f_{adv} = U/D$ of the carrier particles to the

substrate, where *U* is the speed of the travel of the print head and D is the diameter of the carrier particle, determined by the expression $f_{adv} = f_{feed}$, in which case the media particles are applied in the form of a linear chain, whereby when $f_{feed} > f_{adv}$ the media particles are applied in the form of a chain containing a perturbation sequence, and at the imaging stage the identification of a single media particle and/or the media particles is performed on the basis of the generated perturbation sequence. The invention also includes a device for generating carrier particles.

**[0016]** The method described above (Polish patent application P.433162 [42]) allows for printing of aqueous droplets under an external fluorinated fluid phase where a non-fluorinated oil (e.g., hexadecane, or silicone oil, or mixtures thereof) is used to generate the droplets. However, the method is not directly applicable to the case with aqueous inner and external phases, whereas such a choice is necessary to sustain a long-term culture of cells inside the droplets. In fact, the use of inner and external aqueous phases of same composition (e.g., culture medium) normally leads to an instability, wherein the chain, shortly after printing, spontaneously collapses into a more compact structure under the interfacial tension.

**[0017]** Overall, the currently available methods of droplet labelling suffer from either complexity, low biocompatibility, low throughput or stability issues. In addition, none of the available microfluidic printing or trapping methods have actually been demonstrated to operate directly under an external aqueous environment, e.g., cell culture medium, that is without the necessity of replacement of the external phase by the medium for the purpose of long-term cell culture applications.

**[0018]** First object of the invention is device for printing ordered arrays of double-emulsion droplets at a substrate under an external aqueous phase comprising a movable printing system comprising a movable stage in Y direction and an application system, and the application system comprises an actuator movable in X-Z directions to which a print head is attached wherein the print head is fluidly connected to the source of a dispersed phase and at least one source of dispersing phase, where the printhead comprises a dispersed phase inlet, at least one dispersant phase inlet, and the inlets are fluidly connected to an outlet channel connected to a chamber for attaching an application needle, characterised in that the chamber for attaching the application needle is parallel and coaxial or perpendicular to the outlet channel, wherein inner surface of the needle is rendered hydrophobic, preferably fluorophilic, wherein outer surface of the needle is susceptible to wetting by the external phase, and the movable stage comprises a substrate with a modified surface for dispensing a train of monodisperse double-emulsion droplets, being carrier particles.

**[0019]** Preferably the surface of the substrate is modified by laser ablation, sandblasting or made by coping laser-ablated substrate in polydimethylsiloxane. Preferably the substrate is made of glass. polydimethylsiloxane, polytetrafluoroethylene or tetrafluoroethylene-hexafluoropropylene-vinylidenefluoride copolymer.

**[0020]** Preferably, the surface of substrate is modified to increase its roughness coefficient when compared to non-modified substrate. Preferably, the substrate is covered with fluoropolymer-based coating.

**[0021]** Preferably, the dispersed phase inlet channel, at least one dispersant phase inlet channel are connected at right angle. Preferably, height of the inlet channels and of the outlet channel equals their width.

**[0022]** In another preferable embodiment the device comprises one, two or three inlets of the dispersed phase, wherein one inlet is fluidly connected with channel with channel thus forming T-junction, wherein two or three inlets are fluidly connected with channels forming Y-junction from which encompasses channel fluidly connected with channel thus forming T-junction.

**[0023]** Another object of the invention is a method of printing ordered arrays of double-emulsion droplets on a substrate under an external phase, where suspension of the droplets is generated and applied on a substrate under the external aqueous phase, comprising provision of the device, adjusting and putting into linear motion print head against the substrate, generation of the double-emulsion droplets from at least one dispersed phase and dispersing phase, optionally in the generated droplets cells are incapsulated, and extrusion of the droplets on the substrate, characterised in that, the droplets are extruded through a needle with inner diameter $D_{in}$, and diameter of the single droplet D obeys $D>w$ and $D > D_{in}$, where w is height of the inlet channels, where flow rate of the dispersed phase and the dispersing phase is from 3 to 7 μL/min and 10 to 30 μL/min, respectively, preferably the flow rate is constant to generate the droplets of constant diameter, wherein the print head moves with speed of 20 mm/s to 25mm/s versus the substrate, wherein distance d of the needle's tip from the substrate is from $d>D$ to $d<D$, preferably $d=D$, whereas the droplets are generated extruded simultaneously with the translation of the print head, and the external phase comprises surfactant with concentration below critical micelle concentration from 0.001% w/w to 0.1% w/w.

**[0024]** Preferably, the double-emulsion comprises inner aqueous phase/middle phase/external phase, where the inner aqueous phase comprises water or DMEM, minimal essential medium, phosphate-buffered saline or their aqueous solution, the middle phase comprises a fluorinated hydrocarbon, preferably selected from group comprising a solution of Novec 7500 with 2-3% w/w of PFPE-PEG-PFPE fluorosurfactant, the external phase comprises water, DMEM, minimal essential medium, phosphate-buffered saline or their aqueous solution.

**[0025]** Preferably, the surfactant is selected from group comprising: sodium dodecyl sulphate, Pluronic 127, or PFPE-PEG-PFPE fluorosurfactant, preferably sodium dodecyl sulphate or Pluronic 127, wherein the preferable surfactant concentration is 0.1% w/w.

**[0026]** Preferably, flow rate ratio of fluorinated phase:inner aqueous phase is from 1:3 to 1:7, preferably 1:7, preferably ordered arrays of the double-emulsion droplets are printed in linear order.

**[0027]** Preferably, when for generating the double-emulsion droplets at least two dispersed phases are used the droplets are printed with variable flow rate ratio of the dispersed phases comprising variable concentration of an encapsulated substance, preferably varying in a gradual manner, wherein the total flow rate of the dispersed phases is constant.

**[0028]** Further object of the invention is use of the device printing ordered arrays of double-emulsion droplets on a substrate under an external aqueous phase, wherein the droplets may comprise constant or varying concentration of an encapsulated substance.

**The essence of the invention**

**[0029]** The invention describes a method which allows extrusion-printing of aqueous droplets generated at a high volume fraction in an immiscible carrier phase using microfluidics -Polish patent application P.433162 [42]- at a substrate submerged in an external aqueous bath. The essence of the invention consists in the proper modification of the substrate which allows for rapid spreading of the carrier phase at the substrate immediately upon extrusion of the droplets. This is achieved via optimal roughening of the substrate resulting in surface of well defined microporosity and via chemical modification of the substrate rendering its affinity towards the carrier phase, preferably a fluorinated fluid. The method allows for printing of highly stable close-packed chains of aqueous droplets at a substrate submerged under an external aqueous bath, that is printing of a double-emulsion W/F/W droplet-chain, where 'F' denotes the fluorinated fluid **(Figure 1 a,b).** Stability of the chain relies on spontaneous self-ordering of the droplets into a linear structure under capillary forces imposed by the encapsulating fluorinated phase, supplied at a very low volume fraction [43], without the use of any prefabricated wells or traps. The use of the optimally roughened substrate warrants capillary arrest and long-term stability of the printed droplet structure.

**[0030]** As the printing needle moves along the substrate, the subsequent aqueous droplets are extruded and transferred to the substrate without breaking the continuity of the encapsulating fluorinated fluid phase resulting in the formation of a chain of droplets connected by capillary bridges of the fluorinated fluid **(Figure 1 b-e).** The use of a substrate with an optimal high roughness coefficient results in rapid spreading of the fluorinated fluid at the substrate. In addition, the substrate microporosity results in partial absorption of the fluorinated phase which enhances capillary arrest of the droplets, stabilizing the printed structure long after printing. The substrates of optimal roughness and microporosity are obtained via laser ablation of the standard glass substrates under well-defined conditions of the ablation process. In particular, a 30 W sealed $CO_2$ laser (Laser Pro C180II, GCC, Taiwan) is used to ablate the standard 1 mm thick borosilicate glass slide under the conditions of power 3.0 W per laser pulse, engraving speed 1.0 IPS (inch per second) and pulse rate 500 PPI (pulse per inch). The fabricated rough substrate allows extrusion-printing of long-term stable W/F/W droplet chains **(Figure 1 f-h**).

**[0031]** The incubation of the ordered array of the W/F/W emulsion droplets printed at a substrate has several advantages as compared to other methods of droplet storage, incubation and ordering on-chip or off-chip. Those advantages include (i) simplicity and low cost (no need for specially prefabricated traps), (ii) high-throughput of droplet deposition (at least 10 droplets/s, possibly 100 droplets/s or more), (iii) efficient clos-packing of the droplets at the substrate (due to their close-packing in the chain), (iv) possibility of droplet identification without injection of dyes or other 'barcodes', based solely on the sequential deposition of the droplets at the substrate and on the self-assembled local patterns, and (v) the possibility of printing 'in-situ' under cell culture media, i.e., without the need for the external phase replacement after printing.

**The choice of fluids in the double-emulsion W/F/W droplet printing experiments**

**[0032]** The preferred selection of fluids comprising the double-emulsion system for applications in cell culture, high throughput screening or tissue engineering typically consists of an inner aqueous phase, a middle oil phase, and an external aqueous phase, i.e., a W/O/W core-shell system with an aqueous core engulfed by an oil shell and suspended in external aqueous environment (water, basal medium, etc.) [6].

**[0033]** The middle oil phase should be a biocompatible oil-surfactant mixture. Several studies have reported the use of fluorinated fluids such as FC-40 (3M, USA) and Novec 7500 (3M, USA, CAS No. 297730-93-9) as the external or middle oil phase forming W/F or W/F/W systems, respectively, capable of encapsulating and culturing living cells. In particular, fluorinated fluids have been found to be gas-permeable [9], [10], [46] allowing supply of oxygen to the cells encapsulated in the aqueous or hydrogel cores. The surfactant provides the stability of the emulsion via forming a dense monolayer at the droplet interfaces. In particular, in W/F/W double-emulsions, the surfactant prevents the escape of the inner aqueous droplet outside of the fluorinated 'shell'. During the experiments, the perfluoropolyether-polyethylene glycol perfluoropolyether (PFPE-PEG-PFPE) block copolymer surfactant (Chemipan, Poland) synthesized according to the method described in references [47] and [48] was used at 3% w/w concentration.

**[0034]** Regarding the stability of the printed double-emulsion chains of aqueous droplets, based on the previous

literature [43], one can assume that the interfacial energies between the fluorinated fluid and the external phase $\gamma_{ext}$ and between the fluorinated fluid and the inner phase $\gamma_{in}$ must obey $\gamma_{ext} < \gamma_{in}$. Therefore, a simple way of warranting the stability of chains in a W/F/W system is the addition of a hydrophilic surfactant to the external aqueous phase such that it lowers $\gamma_{ext}$ without affecting $\gamma_{in}$. Preferably, the surfactant can be sodium dodecyl sulfate (SDS, Merck, USA, CAS No. 151-21-3) [49] or Pluronic F127 (CAS No. 9003-11-6) [50], [51]. A precise control over the surfactant concentration in the external aqueous phase and optimization of the surface roughness/microporosity are crucial in achieving stable one-by-one droplet deposition and the stability of the printed structure. In the case without any surfactant or at low SDS surfactant concentrations in the external aqueous phase, i.e., well below the CMC (critical micelle concentration), the use of a smooth glass substrate results in gradual collapse of a printed chain into a double-chain or even more compact structures **(Figure** 2b).

**[0035]** With the same set of fluids, the use of an optimally roughened substrate prevents the collapse during and after printing. There are only occasional rearrangements happening within tens of seconds after printing **(Figure** 2c). In this case, the droplets appear deformed due to the interfacial tension $\gamma_{ext}$ being equal or close to $\gamma_{in}$.

**[0036]** Droplet deformation is significantly reduced at higher SDS concentrations. However, when the SDS concentration exceeds the CMC one observes sliding of the extruded W/F emulsion at the substrate **(Figure 2a).** The sliding phenomenon may be associated with the presence of SDS micelles in the external aqueous phase [52] which prevent or delay the rupture of the aqueous film beneath the extruded double-emulsion droplets. Noteworthy, the use of a rough substrate does not eliminate the sliding phenomenon. In addition, as the interfacial tension $\gamma_{ext}$ drops roughly below 3 mN/m, the extruded structures, subject to viscous friction at the substrate, loose their integrity and break into a series of separated clusters or even separated individual droplets. This type of instability may be attributed to the weakness of the binding capillary forces owing to the excessively low interfacial tension $\gamma_{ext}$.

**[0037]** The optimal printing conditions can be associated with the use of a rough substrate obtained via laser ablation of borosilicate glass at optimized conditions, with an average roughness of approximately 10 $\mu$m and at the SDS concentration just below CMC, preferably 0.1% w/w **(Figure 2d).** In such a case, the structures are efficiently transferred to the substrate and there are no post-printing rearrangements. Also, in this case, the droplets appear much less deformed as compared to the case without surfactant or at significantly lower SDS concentrations 0.01% or 0.001% w/w. In the case of rough substrates obtained via laser ablation at sub-optimal conditions, or in the case of commercial opaque (rough) glass slides, the stabilization of the printed structures is less efficient and typically one observes some rearrangements at least within minutes after printing (see **Example 1**).

**[0038]** The table in **Figure 2 e-f** summarizes findings for all SDS and Pluronic surfactant concentrations tested. In **Figure 2g** plot the interfacial tensions between an aqueous solution of SDS or Pluronic F-127 [53] and Novec 7500 with 3% w/w PFPE-PEG-PFPE fluorosurfactant, measured via pendant-drop method is presented.

**Droplet printing setup**

**[0039]** The droplet printing setup is assembled according the invention described in the Polish patent application P.433162 [42] and compriese an automate XYZ stage, a microfluidic printhead connected to a syringe pump (or other flow supply) and terminating with a printing needle, and a substrate at which the droplets are printed, submerged in an aqueous bath **(Figure 1a).** In the current study, besides a simple T-junction **(Figure 1f,g**), another chip comprising a Y-junction **(Figure 1h)** or a psi-junction **(Figure 1i)** upstream the T-junction are described. High-order junctions with multiple inlet channels and a single outlet channel are also possible. Additionally, a method of connecting the outlet needle in the direction perpendicular to the chip **(Figure 1g)** is introduced. Such configuration facilitates simultaneous monitoring of the processes of droplet generation at the chip and of the droplet transfer to the substrate with the use of a single camera mounted at the printhead.

**Laser ablation**

**[0040]** Among several methods of substrate roughening, laser ablation leads to substrates that particularly well support the stability of the chains of droplets. Nowadays, lasers are commonly employed to create intricate three-dimensional microstructures that find various applications in fields like optics, optoelectronics, semiconductors, and microfluidics [54]. A focused laser beam can generate highly localized thermal gradients by sending multiple focused pulses in short periods of time **(Figure 3a,b).** In the present invention, a commercial laser engraving machine (Laser Pro C180II, GCC, Taiwan) equipped with a 30 W sealed $CO_2$ laser was used, emitting infrared laser pulses of wavelength 10.6 $\mu$m. The device is equipped with an adjustable power control supplying a dynamic range of power from 0 to 30 W for each laser pulse fired. The laser-engraving process leads to generation of intricate patterns consisting of numerous small-scale imperfections or cracks, which vary in their specific structure based on the frequency of the laser pulses. Apart from the power, the final characteristics of the patterns depend on the applied power as well as on the surface density of the ablated spots which can be controlled by adjusting (i) the pulse frequency in the range of 30 to 1500 PPI (pulses per inch) and the speed of the

projected laser beam or the 'engraving speed' in the range of 0.04 to 40 IPS (inches per second) [55].

**Roughness measurements**

**[0041]** The surface topography and roughness of the substrates were measured using optical profilometry with vertical and lateral resolutions of 1 nm and 200-500 nm, respectively [56] **(Figure 3c,d).** According to the ASME B46.1-2009 standard, "Surface Texture (Surface Roughness, Waviness, and Lay)", the *root mean square roughness R* was used as the measure of roughness, defined as the standard deviation of the profile *Z(x,y)* over the probed area. Considering a square area of dimensions L x L, the root mean square roughness R can be calculated as

$$R = \left[\frac{1}{L^2}\int_0^L dx \int_0^L dy(\Delta Z(x,y))^2\right]^{\frac{1}{2}} \quad \text{(I)}$$

where

$$\Delta Z(x,y) = Z(x,y) - Z_0$$

is the deviation of the profile relative to the mean elevation $Z_0$, with

$$Z_0 = \frac{1}{L^2}\int_0^L dx \int_0^L dy\, Z(x,y). \quad \text{(II)}$$

Numerically, R is calculated as:

$$R = [(\Delta Z_1^2 + \Delta Z_2^2 + \Delta Z_3^2 + \cdots + \Delta Z_n^2)/n]^{1/2}, \quad \text{(III)}$$

where n is the number of the sampled spots [57].

**[0042]** The measurements were performed using randomly selected 1 × 1 mm areas of the substrates using a commercial optical profilometer (ContourGT, Bruker, USA).

**Droplet deposition at various types of substrates including rough substrates**

**[0043]** It was expected that a rapid drainage of the lubricating film underneath a droplet in the case of a rough substrate is likely associated with the enhanced variations in local film thickness which induce the stochastic rupture. In fact, even in the case of the non-rough substrates [58], [59], down to the atomically smooth ones [60], [61], the dynamics of film rupture, quantified in terms of the drainage time $t_{drain}$, defined as the lag time between the formation of the film and its rupture [62], has been reported to be stochastic. Accordingly, one would anticipate that the added roughness further enhances the stochastic rupture, thus reducing the drainage time.

**[0044]** To assess the influence of surface roughness on droplet spreading dynamics, a simplified system was employed. In this system, a fluorinated fluid droplet, suspended in an external pure water phase (F-in-W emulsion), was delicately deposited onto glass substrates with varying roughness **(Figure 4a,b).** The drainage time ($t_{drain}$) of the aqueous film developing beneath the droplet was measured, with the moment of film rupture identified as the time of an abrupt change in the measured droplet width. The measurements were conducted for:

(i) smooth glass substrates (So),
(ii) commercial rough (opaque) glass plates ($S_{dif1}$ and $S_{dif2}$) as well as
(iii) custom substrates prepared using various types of roughening methods including laser ablation ($S_1$, $S_2$, $S_3$, $S_4$, $S_5$, $S_{opt}$) and sandblasting ($S_{sand}$, $S_{THV,sand}$ and $S_{PTFE,sand}$).

**[0045]** It was determined that rougher substrates (higher R) correlate with faster droplet spreading, i.e., shorter drainage time $t_{drain}$ **(Figure 4c).**

**[0046]** Finally, the stability of droplet lines printed on substrates composed of various materials, including glass, PDMS (poly dimethylsiloxane; CAS 9016-00-6), and transparent fluoropolymers such as PTFE (polytetrafluoroethylene; CAS 9002-84-0 and THV (tetrafluoroethylene-hexafluoropropylene-vinylidenefluoride copolymer; CAS 25190-89-0), was also examined. These substrates were either master-molded from rough glass substrates (PDMS) or roughened through

sandblasting after molding from smooth substrates (PTFE, THV). It was observed that the greatest stability was attained when utilizing laser-ablated glass substrates roughened under optimal engraving parameters.

**Needle modification in the double-emulsion W/F/W droplet printing experiments**

**[0047]** During the printing of the emulsion droplets under an external aqueous phase, with a fluorinated fluid Novec 7500 as the middle phase, the inner aqueous droplets-instead of being transferred to the substrate-may migrate, due to buoyancy, upward, along the external surface of the outlet needle (Novec 7500 density is 1.625 g/cm$^3$, which is much greater than water). In the W/F/W system, the problem is particularly pronounced in the case when the outer surface of the needle is preferentially wetted by the fluorinated phase **(Figure 5a).** In such a case the fluorinated fluid may form a pocket at the outer surface of the needle (close to the tip) accommodating multiple aqueous droplets and so preventing their transfer to the substrate. To avoid this problem, the outer surface of the needle should be preferentially wetted by the external phase **(Figure 5b).** In the case of W/F/W systems, this means that it should be rendered hydrophilic. At the same time, since the fluorinated phase is carrying the droplets inside the needle, the inner surface of the needle should remain hydrophobic and preferentially fluorophilic. Preferentially, one uses a stainless-steel needle which preferentially can be a blunt 25G needle (0.52 mm outer diameter), and modify the inner surface of the needle fluorophilic via applying a fluoropolymer-based coating (Novec 1720, 3M, USA). To this end, the needle is connected to an inlet and outlet tubing, which supplies the coating agent and prevents modification of the outer surface. The needle is left for drying and curing at 120 °C for 20 mins. On the outside, the hydrophilicity is retained via cleaning with isopropanol, whereas the needle tips are blocked to avoid contact of the inner walls with isopropanol. In such a way, a needle with fluorophilic inner surface and hydrophilic outer surface is achieved.

**[0048]** The important tunable parameter during the printing process is the distance *d* **(Figure 1b)** between the needle tip and the substrate. As described in the Polish patent application P.433162 [42], this distance should be finely adjusted to match the diameter *D* of the extruded droplets **(Figure 1c)** [63] in order to avoid droplet splitting ($d<D$) or droplet sliding and/or accumulation at the needle ($d>D$).

**[0049]** Overall, a successful printing of stable droplet chains is only possible with the use of (i) the external aqueous phase with added surfactant at optimal sub-CMC concentration, (ii) an optimally roughened substrate, (iii) a modified needle with a hydrophobic (fluorophilic) inner wall and a hydrophilic outer wall, and (iv) with the fine-tuned gap size d = D.

**[0050]** Preferred examples of embodiments are now explained with reference to the accompanying figures, wherein:

Fig. 1 explains the generation and direct-printing of double-emulsion droplet-chains on a substrate, a) Schematics of the setup including a syringe pump or other source of pressure (1), the middle liquid phase (2), the inner liquid phase (3), elastic tubing (4), a microfluidic chip (5), a T-junction (6) allowing generation of monodisperse microdroplets in the outlet channel (7), a motorized XZ-actuator (8), an outlet needle (9), a rough transparent substrate (10), the external liquid phase (11), a transparent container for the external phase (12), the extruded droplet-chain (13), a motorized Y-stage (14). b) Side-view (alongthe y-direction) of the printed double-emulsion droplet-chain showing the placement of the needle tip at a distance d above the substrate. c) Left panel: close-up view (same as in 'b') with indicated morphology of the capillary bridges between the droplets. Right panel: cross-section (along the x-direction) of the chain showing a meniscus of the oil phase between the droplet and the substrate responsible for capillary adhesion. d, e) Typical large-scale morphologies of the printed chain: a straight chain (d) achievable for $U_x = Df_{gen}$, where $f_{gen}$ is the frequency of droplet generation, and partially folded chain (e) achievable for $Df_{gen} < U_x < 2Df_{gen}$. f-h) Schematics of the microfluidic chips: f) upper and lower panels: top and side view, respectively, of a microfluidic chip consisting of two polycarbonate rectangular slides (5) with micromilled channels of height h and width w, a T-junction (6) connecting the inlet channels (7a) and (7b), an outlet channel (7), an outlet port (15) for accommodating the outlet needle (9), an inlet port for the continuous phase (16), and an inlet port for the dispersed phase (17). Note that the inner diameter $D_1$ of the outlet needle must obey $D_1 > h$ and the needle must be precisely aligned with the outlet port (15); g) Upper and lower panels: top and side view of a microfluidic chip similar to the one depicted in panel in (f) but with the outlet port (15) and outlet needle (9) directed perpendicular to the outlet channel (7); h) schematic of a microfluidic Y-junction (6a) connecting two different inlet ports for the dispersed phase (17a,b) into one channel connected serially to a T-junction (6), suitable for generation of droplets with a changing concentration of a substance (e.g., a drug) supplied to one of the inlet ports (17a,b) along the printed line; (i) schematic of a microfluidic Psi-junction (6a) connecting three different inlet ports for the dispersed phase (17a-c) into one channel connected serially to a T-junction (6), suitable for applications such as screening of the impact of a changing concentration of a substance (a drug) supplied to one of the two inlets (e.g., 17a,b) on cells co-encapsulated inside the droplets and supplied to the third inlet (e.g., 17c). j-l) Snapshots of the droplet-chains during printing (j) and after printing (k,l), including side-view (j,k) and top-view (l).

Fig. 2 displays (a) time-series of top-view snapshots of the printed droplet structures for various concentrations [C] of the SDS in the external aqueous phase W, and (b) impact of the two different surfactants (SDS and Pluronic F-127) and their concentrations on the interfacial tension of the F/W interface as measured using pendant-drop method (within 5-10 s after droplet formation). Note: The snapshots in the categories 'complete sliding', 'stable threads with deformed droplets', and 'stable threads' have been taken in the case with optimally roughened substrate $S_{opt}$. The snapshots in the category 'complete folding' have been taken in the case with a smooth glass substrate So.

Fig. 3 depicts the principle of laser ablation resulting in roughened glass substrates suitable for the deposition of long-term stable double-emulsion droplet-chains. a) Schematic of the laser engraver including the $CO_2$ laser source (18), mirrors (19), objective (20), and the glass substrate (21). b) Optical-microscopic view (22) of the roughened glass substrate. c) Surface profile *Z(x,y)* of the glass substrate (here, $S_{opt}$) acquired using white-light interference optical profilometry (field of view L x *L* = 1 mm x 1 mm). d) Section Z(x) of the surface profile shown in (c) for a fixed *y* (*y* = 0.5 mm);

Fig. 4 illustrates the drainage of a thin film of an external liquid phase, composed of an 80% w/w aqueous glycerin solution, trapped under a quasi-spherical droplet of fluorinated fluid Novec 7500 gently deposited on two types of glass substrates, (a) smooth ($S_0$) and (b) rough ($S_{opt}$). c) The measured drainage time as a function of the substrate roughness R (measured using optical profilometry) for the smooth substrate $S_0$ , commercial rough substrates ($S_{dif1}$, $S_{dif2}$) and the different laser ablated substrates ($S_1$, $S_2$, $S_3$, $S_4$, $S_5$, $S_{opt}$).

Fig. 5 provides a schematic and snapshots of an outlet needle (treated on the outside with oxygen plasma and on the inside with the fluorophilic coating Novec 1720) and shows the behavior of the extruded aqueous droplets in two situations: before and after cleaning of the outer surface of the needle from oil residues (the oil is Novec 7500) using isopropanol. a) Undesired situation with a droplet migrating upwards at the outer surface of the needle. b) Desired situation with an aqueous droplet pending at the tip of the needle.

Fig. 6 shows optical profilometry scans of the different tested substrates and a time-series of snapshots of the printed droplet chains illustrating the stability of the chain at late times after printing for the cases of a) the smooth substrate (So), and b) the commercial roughened glass substrate 'diffuser 1' ($S_{dif1}$).

Fig. 7 same as Fig. 5 for the cases of a) the commercial roughened glass substrate 'diffuser 2' ($S_{dif2}$), and b) laser ablated 'optimal' glass substrate ($S_{opt}$).

Fig. 8 shows the different measured average roughnesses R of the laser-ablated glass substrates as a function of the $CO_2$ laser power and the laser PPI.

Fig. 9 provides snapshots of the droplet chain immediately after printing (t = 0s, upper row) and 2 min after printing (t = 120s, lower row) in the cases of various types of rough substrates: sandblasted glass ($S_{sand}$), sandblasted THV ($S_{THV,sand}$), sandblasted PTFE ($S_{PTFE,sand}$), PDMS copy of $S_{dif2}$ ($S_{dif2,PDMS}$), commercial roughened glass ($S_{dif2}$) and laser ablated glass ($S_{opt}$).

Fig. 10 presents a bar graph depicting the surface roughness measurements of various tested materials following a successful droplet transfer to the substrate. The materials included in the study were sandblasted glass, THV, and PTFE; additionally, PDMS copies of commercial diffusor 2 ($S_{dif2}$) were prepared. Notably, the PDMS copy of $S_{dif2}$, that is $S_{dif2\_PDMS}$, stands out with a 40% increase in surface roughness compared to its original sample. This significant rise in surface roughness can be attributed to the silanization reaction that took place on the polymerized PDMS surface, a phenomenon discussed in previous literature [64].

Fig. 11 shows time-series of snapshots of a M/F/M double-emulsion droplet chain with the droplet's inner and the external phases being basal medium (M) (Dulbecco's Modified Eagle's Medium, DMEM, Gibco, ThermoFisher Scientific, USA. CAS No. 12660012) printed at (a) the commercial rough substrate ($S_{dif2}$) and (b) the laser ablated substrate ($S_{opt}$) illustrating the stability of the chain after printing. The inner phase was additionally colored with phenol red (150 mg/L). The middle phase (F) comprised the same mixture of Novec 7500 and PFPE-PEG-PFPE surfactant described before, whereas the external phase had added Pluronic-F-127 surfactant at 0.1% w/w concentration.

Fig. 12 presents an application involving the generation of droplets containing a gradually decreasing concentration of a dye (Erioglaucine sodium salt, the blue dye) and a gradually increasing concentration of another dye (150 mg/L phenol red, the red dye) along the printed droplet chain. The process utilizes a Y-junction (6a) to control the concentration of the two substances inside the droplets wherein the syringe pump (2) provides a gradually changing rates of flow of the two to-be dispersed aqueous phases via two syringes connected to the two inlets of the Y-junction, however, such that the net rate of flow of both aqueous phases remains constant over time, and so does the rate of flow of the oil phase (see the plot in the top left corner).

Fig. 13 illustrates a time series capturing experimental snapshots taken over 24 hours. The snapshots depict a chain of droplets at an optimal rough substrate $S_{opt}$. Notably, the structural integrity of the droplet chain remains predominantly unchanged even after 24-hours. One can observe isolated rearrangements of around 5% of droplets and coalescence of around 1% of them.

**Example 1: printing of the double-emulsion W/F/W droplets at laser-ablated glass substrates**

**[0051]** The T-junction chip with perpendicular outlet needle **(Figure 1g)** was mounted at a 3D printer arm (8) (3Novatica, Poland), allowing movement in X, Y, and Z axes **(Figure 1a).** In this experiment, and following ones, the printing speeds ranging from 20 to 25 mm/s were used. In all examples, the high-precision syringe pumps (1) (neMESYS 290N, Cetoni GmbH, Germany) were used to inject liquids onto the microfluidic chip (5) at flow rates ranging from 3 to 7 μL/min for the fluorinated fluid and from 10 to 30 μL/min for the aqueous phase.

**[0052]** The droplets were generated at a T-junction (6) of channels of a square cross-section and of the width $w = 150$ μm and the same height $h = w$. The droplets were subsequently transported via an outlet channel (7) towards an outlet 25G needle (9) of the inner diameter equal $D_1 = 260$ μm. To enable the sequential extrusion of the droplets, the droplet volume was such that the droplets formed plugs confined by the inner walls of the channel and of the inner wall of the needle. This requirement was equivalent to the condition that the diameter $D$ of a free (spherical) droplet obeyed $D > w$ and $D > D_1$. In our experimental setup the inner needle diameter was larger than channel width, $D_1 > w$, so the condition on droplet size $D > D_1$ was sufficient. When it was fulfilled, the droplets formed a 'train' (13) of evenly spaced plugs inside the needle and they could be extruded at a regular frequency one-by-one, while avoiding chaotic collisions with the other droplets.

**[0053]** Prior to supplying the flows of oil and the dispersed phases by the syringe pump, the printhead moves in the Z-direction (8) down until adjusting the gap d between the needle tip and the substrate (10) such that $d = D$. Then, the droplet generation and extrusion is initiated simultaneously with the translation of the printhead in the x-direction such that the droplets are extruded one-by-one onto the substrate forming a chain stabilized by capillary bridges of the oil phase **(Figure 1b-e).**

**[0054]** The volume fraction of the droplets ($\phi$) was set by the applied rates of flow of the water and fluorinated fluid phases $Q_W$, $Q_F$, respectively, where $\phi = Q_W/(Q_F+Q_W)$. In order to print stable chains of droplets the volume fraction $\phi$ must have fulfilled the following two requirements. First, the condition that the droplets form plugs, according to the droplet size scaling for a T-junction reported in Ref. [65], could be expressed as $\phi > \phi_{plug}$, with $\phi_{plug} = 1-(6/\pi)(w/D_1)^3$, which in our case corresponded to $\phi_{plug} = 0.63$. Second, the condition for capillary arrest of the droplet chain at the substrate $\phi > \phi_{arrest}$, which in general depends on the type of substrate. It has been experimentally established the critical volume fraction to be around $\phi_{arrest} = 0.75$ for the rough substrate $S_{opt}$. In the case of less rough substrates it is expected $\phi_{arrest}$ to further increase and, in the case of the smooth glass substrate So, to reach a value close to unity which means that it is practically impossible to print stable lines at smooth substrates. In fact, the actual maximum applicable volume fraction $\phi_{max}$ is associated with an increasing tendency of the droplets to coalesce upon extrusion from the needle upon $\phi$ approaching $\phi_{max}$. This upper limit in our system was estimated to be around $\phi_{max} = 0.9$. The coalescence issues are presumably caused by the rapid expansion of the droplet interface upon its extrusion which in turn results in insufficient coverage of the droplet interface with the PFPE-PEG-PFPE fluorosurfactant. In all of the printing experiments, as described below, $\phi = 0.875$ was always used with the flow rates 4 μL/min : 28 μL/min (fluorinated phase : aqueous phase). In this case, the size of the droplets was around D = 450 μm with a typical coefficient of variation CV ≈ 7%.

**[0055]** The preferred volume fraction $\phi = 0.875$ corresponds to the flow rate ratio 1:7 (fluorinated phase:aqueous phase). In this case, the possible flow rates are, for example 3 μL/min:21 μL/min, or 4 μL/min:28 μL/min. Other possible flow rates are the following: (ratio 1:6) 3 μL/min:18 μL/min, 4 μL/min:24 μL/min, or 5 μL/min:30 μL/min; (ratio 1:5) 3 μL/min:15 μL/min, 4 μL/min : 20 μL/min, 5 μL/min:25 μL/min, or 6 μL/min:30 μL/min; (ratio 1:4) 3 μL/min:12 μL/min, 4 μL/min:16 μL/min, 5 μL/min:20 μL/min, 6 μL/min:24 μL/min, or 7 μL/min:28 μL/min; (ratio 1:3) 3 μL/min:9 μL/min, or 4 μL/min:12 μL/min, 5 μL/min:15 μL/min, 6 μL/min:18 μL/min, or 7 μL/min:21 μL/min.

**[0056]** First, various types of glass substrates were used, that is, in particular, 1mm-thick borosilicate smooth glass slide ($S_0$), moderately rough diffuse glass substrates ($S_{dif1}$), highly rough diffuse glass substrate ($S_{dif2}$) as well as laser-ablated glass substrates ($S_1$, $S_2$, $S_3$, $S_4$, $S_5$, and $S_{opt}$). All glass substrates were treated with a fluoropolymer-based commercial coating 3M Novec 1720 which rendered the surfaces fluorophilic. The coating was applied via immersion of a glass slide in the liquid agent followed by drying and curing at 135°C [66]. The treatment was performed prior to droplet printing experiments. After cooling, the glass samples were immersed in a transparent container (12) filled with distilled and degassed water with 0.1 % w/w surfactant (SDS). As the inner aqueous phase (3), distilled water with 0.1 % w/w Erioglaucine disodium salt (blue dye) were used. As the middle phase (2), Novec 7500 fluorinated fluid with 3% w/w of PFPE-PEG-PFPE surfactant were used, synthesized according to the protocol provided in Ref. [47], [48].

**[0057]** Among the tested substrates, it was found that the most stable droplet lines can be printed using the laser ablated glass substrates, in particular those with optimized laser-engraving parameters ($S_{opt}$). To demonstrate the superiority of those substrates, the results for droplet-line printing at various types of substrates including non-optimally roughened glass plates as well as other (non-glass) rough substrates were compared.

- **$S_0$ and $S_{dif1}$**. In the case of smooth glass substrates So (1mm-thick borosilicate glass slides) and commercial moderately rough substrates $S_{dif1}$, even upon successful transfer of the droplets to the substrate and the formation of a transiently-stable droplet chain (possible in some cases), the chain eventually collapsed, i.e., a 1-row structure

sequentially rearranged into a 2-row structure **(Figure 6).** Typically, during the collapse of the 1-row structures consisting of 10-20 droplets, the rearrangements happened on average every 1-4 seconds.

- **$S_{dif2}$.** In contrast, in the case of more rough diffuse glass substrates $S_{dif2}$, the rearrangements happened only occasionally within first few tens of seconds after printing and in general did not lead to a complete collapse of 1-row structures **(Figure 7a).**

**[0058]** The glass substrates (1mm-thick borosilicate glass slides) roughened by laser ablation (21), consisted of complex arrays of thousands of micrometric defects or cavities (22) **(Figure 3b-d)** whose exact microstructure depended on the frequency of the pulses [54]. It was observed that excessively high pulse rates (PPI, the number of pulses per inch), power, or engraving speed values resulted in delamination of the ablated section or even occasional cracking of the whole slide. In contrast, too low PPI or power values resulted in substrates of moderate roughness which did not warrant printability/stability of droplet arrays. In most experiments, the onset of delamination corresponded to the power range 3.0 - 4.5 W ('transition zone', see **Figure 8)** at PPI values between 500 and 1500. Additionally, higher laser linear speed (approximately 4.0 IPS) caused a decrease in the laser spot width and as a result more inhomogeneous, anisotropic patterns [55]. To achieve possibly high homogeneity, the spot width was kept relatively large with the laser speed set to 4.0 IPS (inches per second) or lower.

- **$S_1$, $S_2$, $S_3$, $S_4$, and $S_5$.** First, the laser was set at 1500 PPI with a linear speed of 4.0 IPS for all experiments. Next, power values of 1.5, 3.0, 4.5, 6.0, and 7.5 W were tested one by one. The samples developed a topography dominated by cavities, cracks, and other defects produced during the laser ablation and were labeled as $S_1$, $S_2$, $S_3$, $S_4$, and $S_5$ according to the increasing laser power used. The droplets could be successfully printed at the substrates and could form a transiently stable single-row chains. However, in most cases, the chains eventually collapsed into a double-row structure. The collapse was slower than in the cases $S_0$ and $S_{dif1}$.
- **$S_{opt}$.** Laser-engraved glass slides generated using 3.0 W power, 1.0 IPS speed and 500 PPI, are referred to as the 'optimal' ones and labeled as $S_{opt}$. The engraved microstructures in these 'optimal' conditions developed a particularly high fraction of 'spikes' with high aspect ratio resulting in a high average roughness value R. In the case of the substrates $S_{opt}$, no collapse was observed **(Figure 7b)** and the structures remained stable for many hours. In this case the enhanced stability can be attributed to the effective microporosity of the substrate caused by glass micro-cracking and formation of the spiky patterns upon laser the ablation process. Such microstructure could presumably facilitate the drainage of the oil phase from between the droplets thus increasing the strength of their capillary arrest.

**[0059]** In all cases of the laser-ablated glass substrates it was also observed small lateral droplet displacements resulting in slight distortions of the printed chains. This effect was presumably caused by the local inhomogeneities of the laser-ablation in the XY-plane. In the case of $S_{opt}$ the distortions had no impact on the long-term chain stability.

**Example 2: printing of the double-emulsion W/F/W droplets at sandblasted THV and PTFE substrates**

**[0060]** Sandblasting exploits a jet of sand driven by compressed air or steam [67]. Similarly, to laser ablation, sandblasting renders rough substrates **(Figure 9, 10).** To conduct the printing experiments using a fluorinated fluid as the oil phase, THV and PTFE substrates were employed, both of which are natively fluorophilic [59]. The substrates were prepared by cutting samples of each material to dimensions of 5 x 5 x 0.3 cm and then cleaning them thoroughly. A Basic Master sandblaster (Renfert, Germany), which was equipped with a delivery scope of 70-250 μm/25-70 μm, was used along with two nozzles measuring 1.2 mm. To achieve optimal results, a special fused alumina abrasive with a particle size of 90-125 μm (200-115 mesh) was used (Renfert, 99.5% $Al_2O_3$). Each sample, PTFE and THV, were inserted in the blasting chamber, and the abrasive was shot perpendicularly through the nozzles at a distance of 1-2 cm. To treat the whole surface, linear sections were covered one by one assuring a uniform distribution of the blasted abrasive on the sample.

**[0061]** The surface roughness and other relevant metrics are reported in **Figure 9,** showing a successful droplet transfer to the substrate achieved by forming a transiently stable droplet chain. In the case of THV, during the first 120 seconds after printing the rearrangement of the droplets from a single- to double-row structure was only observed in small sections of the chain, typically consisting of 5-10 droplets. The PTFE samples showed no signs of collapse at the same time interval. Overall, the sandblasted fluoroplastics such as THV or PTFE also allow printing of relatively stable droplet chains.

**Example 3: printing of the double-emulsion W/F/W droplets at PDMS copies of rough glass substrates**

**[0062]** Polydimethyl siloxane (PDMS) surfaces were prepared using the commercial diffuser glass slide $S_{dif2}$ as a master. First, a PDMS negative master mold was prepared. The PDMS prepolymer (SYLGARD™ 184 Silicone Elastomer Kit, Dow Corning Corporation, Michigan, United States) was mixed in a 9:1 ratio with the supplied curing agent and degassed using a vacuum pump. The mixture was then poured onto the $S_{dif2}$ glass slide and cured at 80°C for 12 hours.

After removing the glass slide, the obtained PDMS negative master was silanized with trichloro(1H,1H,2H,2H-perfluorooctyl)silane (PFOCTS; Sigma-Aldrich, Saint Louis, Missouri, United States) to facilitate the detachment of the casted PDMS copies. The PDMS prepolymer with the curing agent was poured onto the negative master, degassed and cured at 80°C for the next 4-6 hours. After removing from the master, the positive PDMS copies were treated with NOVEC 1720 and cured at 120°C for 2 hours to render the surface fluorophilic. This procedure was repeated for each copy prepared. The tests showed around 40% increase in the surface roughness of the PDMS copy compared to the original sample ($S_{dif2}$) which can be attributed to the process of salinisation as also reported in previous studies [64].

**[0063]** The findings in **Figures 9 and 10** indicate that the droplet transfer onto PDMS substrate was successful, resulting in a transiently stable droplet chain. The chain displayed some lateral undulations, similar to the behavior reported for $S_{opt}$, followed by local droplet rearrangements, typically involving 5-10 droplets, within the first 120 seconds after printing. Overall, the surface modified PDMS copies of rough substrates can be also used for printing of stable droplet lines which could facilitate industrial applications.

**Example 4: printing of double emulsion M/F/M droplets using aqueous basal medium (M) at rough glass substrates**

**[0064]** To assess the suitability of the invention for applications in cell encapsulation for high-throughput screening of drugs, biomaterials, or other active substances, the inner aqueous phase of the system outlined in Example 1 was replaced with a basal medium (DMEM, Gibco, ThermoFisher Scientific, USA). The inner aqueous phase can also comprise minimal essential medium (MEM) or phosphate-buffered saline (PBS). It also posible to use aqueous solution of these media. To ensure good contrast between the droplets and the external phase, the basal medium (M), or its aqueous solution, used as the droplet phase was colored via adding phenol red dye in the concentration of 150 mg/L. As the middle phase, the Novec 7500 fluorinated fluid mixture with 3% w/w of PFPE-PEG-PFPE surfactant was utilized. Finally, a solution of colorless (no added phenol red) basal medium with 0.1% w/w of Pluronic-127 was used as the external aqueous phase. Similar to the previous examples, the substrates $S_{dif2}$ and $S_{opt}$ were treated with a fluoropolymer-based commercial coating 3M Novec 1720 to render them fluorophilic. The slides were subsequently placed in the container under the external medium (M) and the double-emulsion M/F/M droplets were printed. The printing speed, the volume fraction ($\phi$) and the range of applied rates of flow were kept the same as in the Example 1.

**[0065]** In the case of $S_{dif2}$ substrate, after printing, the printed droplet chain started to slowly, yet gradually collapse into a 2-row structure (depicted in **Figure 11a**). In the case of $S_{opt}$ substrate, the collapse was minimal (a single rearrangement at t = 50 s) and the structure remained stable afterwards, as shown in **Figure 11b.** Accordingly, the results are similar to the case of W/F/W system with 0.1% w/w concentration of SDS in the external aqueous phase. In conclusion, it has been demonstrated that the method can be used to print droplets of basal medium under an external phase, which is also a basal medium with added Pluronic-127 surfactant at a concentration below the critical micelle concentration (CMC).

**Example 5: printing of the double-emulsion W/F/W droplets of varying concentrations of two dyes using laser-ablated glass substrates.**

**[0066]** Droplets with controlled varying concentration can be produced with a simple modification of the typical T-junction. Depending on the experiment, a Y-junction variant can be used, a connection of two inlet ports into one inlet channel **(Figure 1h)** or a Psi-junction variant, a connection of three inlet ports into one inlet channel **(Figure 1i).** In both cases, the chip had one inlet port for the fluorinated fluid phase (16) and two or three different inlet ports for the droplet phase (17a,17b,17c).

**[0067]** In the case of a Y-junction, the inlet ports can provide drug A (17a) and drug B (17b), whereas the ratio of the two drugs in each of the droplets generated at the T-junction, located downstream the Y-junction, can be regulated via adjusting the time-dependent rates of flow $Q_A(t)$, $Q_B(t)$ supplied externally via 2 independent flow supply devices, e.g., syringe pumps or pressure controllers. To warrant the constant size of the generated droplets, the net flow rate of the droplet phase $Q_w(t) = Q_A(t) + Q_B(t)$ must remain constant over time, $Q_w(t) = Q_{w0}$. The concentrations $C_A(t)$ and $C_B(t)$ of the drugs in the droplets printed (deposited) at a time t can be calculated as $C_A(t) = C_{A0}\ Q_A(t\text{-}\Delta t)/Q_{w0}$ and $C_B(t) = C_{B0}\ Q_B(t\text{-}\Delta t)/Q_{w0}$, where $C_{A0}$ and $C_{B0}$ are the stock concentrations inside the syringes. The lag time $\Delta t$ between the time of setting of the flow rates (by the flow supply device) and the time of droplet deposition at the substrate can be calculated as $\Delta t = \Delta t_{delay} + \Delta t_{transport}$ where $\Delta t_{delay}$ is the delay time due to the relaxation of the flow supply system (syringes, tubing) while $\Delta t_{transport}$ is the time of travel of the droplets from the T-junction to the substrate, where the latter can be calculated as $\Delta t_{transport} = (w^2 L_{channel} + \pi D_1^2 L_{needle}/4)/(Q_w + Q_o)$ where $L_{channel}$ is the length of the outlet channel (7) and $L_{needle}$ is the length of the needle (9). In the case of the flow supplied by a syringe pump, $\Delta t_{delay}$ is below 1s, while in the case of the flow supplied by pressure controllers it can be even below 100 ms. The time of travel for $L_{channel}$ = 2 cm and $L_{channel}$ = 3 cm and the net flow rate $Q_w + Q_o$ = 10μL/min is around 5 seconds. Accordingly, typically $\Delta t_{transport} >> \Delta t_{delay}$.

**[0068]** **Figure 12** illustrates a model experiment in which the two inlet ports of the Y-junction are supplied with the

aqueous solutions of a red dye (phenol red at the concentration 150 mg/L) and a blue dye (Erioglaucine sodium salt at the concentration 0.1% w/w). The corresponding flow rates $Q_A(t)$ and $Q_B(t)$ are gradually increasing and decreasing at the same rate such that the net rate of flow of the droplet phase $Q_A(t) + Q_B(t)$ remains constant. The fluorinated fluid phase is also supplied at the constant rate of flow and the generated monodisperse droplets are directly printed onto a modified substrate $S_{opt}$ under an aqueous solution of Pluronic-F127 at 0.1% w/w.

**[0069]** The experimental snapshots capture the printed droplet chain with a visible gradient of concentration of both blue and red dyes along the chain. In addition, **Figure 13** provides a series of temporal snapshots spanning 24 hours, depicting a chain of droplets with gradually evolving concentrations of blue and red dyes. These droplets were printed onto the optimally textured glass substrate $S_{opt}$. The overall structure remained stable even after 24 hours. The system demonstrates potential for diverse screening applications in which two different compounds can be applied at varying concentrations. Noteworthy, this also includes the case with a single compound, e.g., drug A, supplied at a varying concentration, achievable via using a pure buffer ($C_{B0} = 0$) instead of the drug B.

**[0070]** In the case of the Psi-junction **(Figure 1i),** the inlet ports can provide drug A (17a), drug B (17b), and cell suspension C (17c). To warrant the constant average number of cells encapsulated in each droplet, in this case the rate of flow Qc(t) should remain constant over time, Qc(t) = Qco, whereas the concentrations of the drugs can be regulated via adjusting the time-dependent rates of flow $Q_A(t)$, $Q_B(t)$. At the same time, to warrant the constant size of the generated droplets, the net flow rate of the droplet phase $Q_w(t) = Q_A(t) + Q_B(t) + Q_{C0}$ must remain constant over time, $Q_w(t) = Q_{w0}$. Similar to the case of the Y-junction, the concentrations $C_A(t)$ and $C_B(t)$ of the drugs in the droplets printed (deposited) at a time t can be calculated as $C_A(t) = C_{Amax}\ Q_A(t\text{-}\Delta t)/Q_{w0}$ and $C_B(t) = C_{Bmax}\ Q_B(t\text{-}\Delta t)/Q_{w0}$ with the delay time $\Delta t$ explained above.

**Summary and applications**

**[0071]** The present invention comprises of (i) a microfluidic droplet generator mounted at a motorized XYZ-stage, generating water-in-fluorinated fluid emulsion droplets and depositing them one-by-one at a substrate in the form of a stable linear chain, whereas the substrate is submerged under an external aqueous phase, and (ii) a method of substrate modification resulting in an optimally roughened surface with surface microporosity and chemical affinity towards the fluorinated fluid phase (i.e., such that the fluorinated phase preferentially wets the substrate). The use of such substrates (i) facilitates transfer of droplets to the substrate and (ii) warrants long-term stability of the printed droplet-structures at the scale of hours or days. Such long-term stability together with the possibility of direct-printing of the droplets under an external aqueous environment opens way to applications in cell encapsulation and long-term culture, e.g., for the purpose of high-throughput drug screening. The stable arrangement of the droplets in the form of a linear chain allows for identification of the droplets at any time during the culture based on their sequential deposition. The invention also provides a way to stabilize more complex droplet arrangements including lines with local perturbations or 'folds' which can serve as 'barcodes' for labelling of the droplets in the chain, as reported in a previous patent application [63]. The printed droplet libraries comprising hundreds or thousands of droplets can be used to test the effect of active molecules added to the droplets or supplied from the external phase via observing the behavior of the cells encapsulated inside the droplets. In particular, the invention allows to check the impact of culture conditions on the encapsulated cells, e.g., the presence of various biomolecules including the components of the extracellular matrix (fibrin, collagen, Matrigel, etc.) or the co-encapsulated other cell types, on the efficacy or toxicity of a co-encapsulated drug. The method could be used, e.g., in screening of drugs in cancer microenvironments or in personalized cancer medicine as means of developing optimized patient-specific treatments.

**References:**

**[0072]**

[1] Y. Ding, P. D. Howes, and J. Andrew, "Recent Advances in Droplet Micro fl uidics," 2020, doi: 10.1021/acs.analchem.9b05047.

[2] G. M. Whitesides, "The origins and the future of microfluidics," Nature, vol. 442, no. 7101, pp. 368-373, Jul. 2006, doi: 10.1038/NATURE05058.

[3] M. T. Guo, A. Rotem, J. A. Heyman, and D. A. Weitz, "Droplet microfluidics for high-throughput biological assays," Lab Chip, vol. 12, no. 12, pp. 2146-2155, May 2012, doi: 10.1039/C2LC21147E.

[4] P. Zhu and L. Wang, "Microfluidics-Enabled Soft Manufacture of Materials with Tailorable Wettability," Chem. Rev., vol. 122, no. 7, pp. 7010-7060, Apr. 2022, doi: 10.1021/ACS.CHEMREV.1C00530/ASSET/IMAGES/LARGE/CR1C00530_0031.JPEG.

[5] A. D. Aladese and H. H. Jeong, "Recent Developments in 3D Printing of Droplet-Based Microfluidics," Biochip J., vol. 15, no. 4, pp. 313-333, Dec. 2021, doi: 10.1007/S13206-021-00032-1/TABLES/1.

[6] R. Chen, Z. Sun, and D. Chen, "Droplet-based microfluidics for cell encapsulation and delivery," Microfluid. Pharm. Appl. From Nano/Micro Syst. Fabr. to Control. Drug Deliv., pp. 307-335, Jan. 2019, doi: 10.1016/B978-0-12-812659-2.00011-9.

[7] Y. Xing, · Love Li, · Xiaoyu Yu, E. G. Fox, Y. Wang, and J. Oberholzer, "Microfuidic Technology for Evaluating and Preserving Islet Function for Islet Transplant in Type 1 Diabetes," Curr. Transplant. Reports, vol. 1, p. 10, Aug. 2022, doi: 10.1007/s40472-022-00377-y.

[8] W. J. Seeto, Y. Tian, S. Pradhan, D. Minond, and E. A. Lipke, "Droplet Microfluidics-Based Fabrication of Monodisperse Polyethylene glycol)-Fibrinogen Breast Cancer Microspheres for Automated Drug Screening Applications," 2022, doi: 10.1021/acsbiomaterials.2c00285.

[9] A. Prastowo, A. Feuerborn, P. R. Cook, and E. J. Walsh, "Biocompatibility of fluids for multiphase drops-in-drops microfluidics," Biomed. Microdevices, vol. 18, no. 6, pp. 1-9, 2016, doi: 10.1007/s10544-016-0137-0.

[10] A. Prastowo, P. R. Cook, and E. J. Walsh, "Biocompatibility of Sessile Drops as Chambers for Cell Culture," Proc. - 2019 2nd Int. Conf. Bioinformatics, Biotechnol. Biomed. Eng. - Bioinforma. Biomed. Eng. BioMIC 2019, Sep. 2019, doi: 10.1109/BIOMIC48413.2019.9034845.

[11] F. Qu et al., "Double emulsion-pretreated microwell culture for the in vitro production of multicellular spheroids and their in situ analysis," Microsystems Nanoeng. 2021 71, vol. 7, no. 1, pp. 1-12, May 2021, doi: 10.1038/s41378-021-00267-w.

[12] A. Kumar, R. Kaur, V. Kumar, S. Kumar, R. Gehlot, and P. Aggarwal, "New insights into water-in-oil-in-water (W/O/W) double emulsions: Properties, fabrication, instability mechanism, and food applications," Trends Food Sci. Technol., vol. 128, pp. 22-37, Oct. 2022, doi: 10.1016/J.TIFS.2022.07.016.

[13] H. Gudapati, M. Dey, and I. Ozbolat, "A comprehensive review on droplet-based bioprinting: Past, present and future," Biomaterials, vol. 102, pp. 20-42, 2016, doi: 10.1016/j.biomaterials.2016.06.012.

[14] J. K. Nunes, S. S. H. Tsai, J. Wan, and H. A. Stone, "Dripping and jetting in microfluidic multiphase flows applied to particle and fibre synthesis," J. Phys. D. Appl. Phys., vol. 46, no. 11, Mar. 2013, doi: 10.1088/0022-3727/46/11/114002.

[15] P. Garstecki, M. J. Fuerstman, A. Stone, and G. M. Whitesides, "Formation of droplets and bubbles in a microfluidic T-junction - scaling and mechanism of break-up {," pp. 437-446, 2006, doi: 10.1039/b510841a.

[16] J. Guzowski, S. Jakiela, P. M. Korczyk Bc, and P. Garstecki, "Custom tailoring multiple droplets one-by-one + Lab on a Chip," Pol. Akad. Nauk Inst. Chem. Fiz., vol. 13, pp. 4308-4311, 2013, doi: 10.1039/c3lc50841b.

[17] F. M. Galogahi, Y. Zhu, H. An, and N.-T. Nguyen, "Formation of core-shell droplets for the encapsulation of liquid contents," vol. 25, p. 82, 2021, doi: 10.1007/s10404-021-02483-2.

[18] F. M. Galogahi, Y. Zhu, H. An, and N. T. Nguyen, "Core-shell microparticles: Generation approaches and applications," J. Sci. Adv. Mater. Devices, vol. 5, no. 4, pp. 417-435, Dec. 2020, doi: 10.1016/J.JSAMD.2020.09.001.

[19] K. K. Brower et al., "Double emulsion flow cytometry with high-throughput single droplet isolation and nucleic acid recovery," Lab Chip, vol. 20, no. 12, pp. 2062-2074, Jun. 2020, doi: 10.1039/D0LC00261E.

[20] K. K. Brower et al., "Double Emulsion Picoreactors for High-Throughput Single-Cell Encapsulation and Phenotyping via FACS," Anal. Chem., vol. 92, no. 19, pp. 13262-13270, Oct. 2020, doi: 10.1021/ACS.ANALCHEM.OC02499/ASSET/IMAGES/LARGE/ACOC02499_0006.JPEG.

[21] W. Jiang, M. Li, Z. Chen, and K. W. Leong, "Cell-laden microfluidic microgels for tissue regeneration," Lab Chip, vol. 16, no. 23, pp. 4482-4506, Nov. 2016, doi: 10.1039/C6LC01193D.

[22] H. F. Chan, Y. Zhang, Y. P. Ho, Y. L. Chiu, Y. Jung, and K. W. Leong, "Rapid formation of multicellular spheroids in double-emulsion droplets with controllable microenvironment," Sci. Reports 2013 31, vol. 3, no. 1, pp. 1-8, Dec. 2013, doi: 10.1038/srep03462.

[23] S. C. Ramaiahgari et al., "A 3D in vitro model of differentiated HepG2 cell spheroids with improved liver-like properties for repeated dose high-throughput toxicity studies," Arch. Toxicol., vol. 88, no. 5, pp. 1083-1095, Mar. 2014, doi: 10.1007/500204-014-1215-9/FIGURES/7.

[24] G. Etienne, A. Vian, M. Biočanin, B. Deplancke, and E. Amstad, "Cross-talk between emulsion drops: how are hydrophilic reagents transported across oil phases?," *Lab Chip,* vol. 18, p. 3903, 2018, doi: 10.1039/c8lc01000e.

[25] T. A. Duncombe and P. S. Dittrich, "Droplet barcoding: tracking mobile micro-reactors for high-throughput biology," Curr. Opin. Biotechnol., vol. 60, pp. 205-212, Dec. 2019, doi: 10.1016/J.COPBIO.2019.05.004.

[26] E. Brouzes et al., "Droplet microfluidic technology for single-cell high-throughput screening," 2009, doi: 10.1073/pnas.0903542106.

[27] R. F. X. Tomasi, S. Sart, T. Champetier, and C. N. Baroud, "Individual Control and Quantification of 3D Spheroids in a High-Density Microfluidic Droplet Array," Cell Rep., vol. 31, no. 8, p. 107670, May 2020, doi: 10.1016/J.CELREP.2020.107670.

[28] J. Q. Boedicker, L. Li, T. R. Kline, and R. F. Ismagilov, "Detecting bacteria and determining their susceptibility to antibiotics by stochastic confinement in nanoliter droplets using plug-based microfluidics," Lab Chip, vol. 8, no. 8, pp. 1265-1272, Jul. 2008, doi: 10.1039/B804911D.

[29] K. Churski et al., "Rapid screening of antibiotic toxicity in an automated microdroplet system," Lab Chip, vol. 12, no. 9, pp. 1629-1637, Apr. 2012, doi: 10.1039/C2LC21284F.
[30] F. Eduati et al., "A microfluidics platform for combinatorial drug screening on cancer biopsies," Nat. Commun. 2018 91, vol. 9, no. 1, pp. 1-13, Jun. 2018, doi: 10.1038/s41467-018-04919-w.
[31] R. H. Cole et al., "Printed droplet microfluidics for on demand dispensing of picoliter droplets and cells," Proc. Natl. Acad. Sci. U. S. A., vol. 114, no. 33, pp. 8728-8733, 2017, doi: 10.1073/pnas.1704020114.
[32] S. Sakakihara, S. Araki, R. Iino, and H. Noji, "A single-molecule enzymatic assay in a directly accessible femtoliter droplet array," Lab Chip, vol. 10, no. 24, pp. 3355-3362, Dec. 2010, doi: 10.1039/C0LC00062K.
[33] S. K. Küster et al., "Interfacing droplet microfluidics with matrix-assisted laser desorption/ionization mass spectrometry: Label-free content analysis of single droplets," Anal. Chem., vol. 85, no. 3, pp. 1285-1289, Feb. 2013, doi: 10.1021/AC3033189/SUPPL_FILE/AC3033189_SI_002.AVI.
[34] Y. Bai, E. Weibull, H. N. Joensson, and H. Andersson-Svahn, "Interfacing picoliter droplet microfluidics with addressable microliter compartments using fluorescence activated cell sorting," Sensors Actuators B Chem., vol. 194, pp. 249-254, Apr. 2014, doi: 10.1016/J.SNB.2013.12.089.
[35] S. Sart, R. Tomasi, G. Amselem, and C. N. Baroud, "Multiscale cytometry and regulation of 3D cell cultures on a chip," Nat. Commun., vol. 8, no. 1, p. 469, 2017, doi: 10.1038/s41467-017-00475-x.
[36] D. Haidas, M. Napiorkowska, S. Schmitt, and P. S. Dittrich, "Parallel Sampling of Nanoliter Droplet Arrays for Noninvasive Protein Analysis in Discrete Yeast Cultivations by MALDI-MS," Anal. Chem., vol. 92, no. 5, pp. 3810-3818, Mar. 2020, doi: 10.1021/ACS.ANALCHEM.9B05235/ASSET/IMAGES/LARGE/AC9B05235_0005.J-PEG.
[37] X. Li, J. M. Zhang, X. Yi, Z. Huang, P. Lv, and H. Duan, "Multimaterial Microfluidic 3D Printing of Textured Composites with Liquid Inclusions," Adv. Sci., vol. 6, no. 3, pp. 1-7, 2019, doi: 10.1002/advs.201800730.
[38] A. Z. Nelson, B. Kundukad, W. K. Wong, S. A. Khan, and P. S. Doyle, "Embedded droplet printing in yield-stress fluids," Proc. Natl. Acad. Sci. U. S. A., vol. 117, no. 11, pp. 5671-5679, Mar. 2020, doi: 10.1073/PNAS.1919363117/SUPPL_FILE/PNAS. 1919363117. SM04. MP4.
[39] S. Ma, "Microfluidics tubing as a synthesizer for ordered microgel networks Microfluidics tubing as a synthesizer for ordered microgel networks," Soft Matter, vol. 15, no. 19, p. 3848, 2019, doi: 10.1039/c9sm00626e.
[40] L. Zhou et al., "Lipid-Bilayer-Supported 3D Printing of Human Cerebral Cortex Cells Reveals Developmental Interactions," Adv. Mater., vol. 32, no. 31, p. 2002183, Aug. 2020, doi: 10.1002/ADMA.202002183.
[41] A. Alcinesio et al., "Controlled packing and single-droplet resolution of 3D-printed functional synthetic tissues," Nat. Commun., vol. 11, no. 1, p. 2105, 2020, doi: 10.1038/s41467-020-15953-y.
[42] J. Guzowski, M. Constantini, and R. Buda, "Method for labeling monodisperse carrier particles and microfluidic device for generating monodisperse carrier particles," Polish Patent application, P.433162, 2021, https://ewyszukiwarka.pue.uprp.gov.pl/search/pwp-details/P.433162?lng=pl
[43] Y. K. Lai, A. S. Opalski, P. Garstecki, L. Derzsi, and J. Guzowski, "A double-step emulsification device for direct generation of double emulsions," Soft Matter, vol. 18, no. 33, pp. 6157-6166, Aug. 2022, doi: 10.1039/D2SM00327A.
[44] L. Amirifar et al., "Droplet-based microfluidics in biomedical applications," Biofabrication, vol. 14, no. 2, p. 022001, Jan. 2022, doi: 10.1088/1758-5090/AC39A9.
[45] S. M. Giannitelli et al., "Droplet-based microfluidic synthesis of nanogels for controlled drug delivery: tailoring nanomaterial properties via pneumatically actuated flow-focusing junction," Nanoscale, vol. 14, no. 31, pp. 11415-11428, Aug. 2022, doi: 10.1039/D2NR00827K.
[46] C. Li et al., "Under-Oil Autonomously Regulated Oxygen Microenvironments: A Goldilocks Principle-Based Approach for Microscale Cell Culture," Adv. Sci., vol. 9, no. 10, Apr. 2022, doi: 10.1002/ADVS.202104510.
[47] M. W. M. Link, Daniel; Hutchison, Brian; Samuel, "Droplet Libraries (US Patent 2010/0022414 A1)," 2010.
[48] C. Holtze et al., "Biocompatible surfactants for water-in-fluorocarbon emulsions," Lab Chip, vol. 8, no. 10, p. 1632, 2008, doi: 10.1039/b806706f.
[49] J.-C. Baret, "Surfactants in droplet-based microfluidics †," Lab Chip, vol. 12, no. 3, p. 403-664, Feb. 2012 doi: 10.1039/c1lc20582j.
[50] G. Aubry, M. Zhan, and H. Lu, "Hydrogel-droplet microfluidic platform for high-resolution imaging and sorting of early larval Caenorhabditis elegans," Lab Chip, vol. 15, no. 6, p. 1424, Mar. 2015, doi: 10.1039/C4LC01384K.
[51] M. Li et al., "A versatile platform for surface modification of microfluidic droplets," Lab Chip, vol. 17, no. 4, p. 635, Feb. 2017, doi: 10.1039/C7LC00079K.
[52] B. Hammouda, "Temperature Effect on the Nanostructure of SDS Micelles in Water," J. Res. Natl. Inst. Stand. Technol., vol. 118, pp. 151-167, 2013, doi: 10.6028/j res.118.008.
[53] Q. Gao, Q. Liang, F. Yu, J. Xu, Q. Zhao, and B. Sun, "Synthesis and characterization of novel amphiphilic copolymer stearic acid-coupled F127 nanoparticles for nano-technology based drug delivery system," Colloids Surfaces B Biointerfaces, vol. 88, pp. 741-748, 2011, doi: 10.1016/j.colsurfb.2011.08.010.
[54] M. Mirkhalaf, A. K. Dastjerdi, and F. Barthelat, "Overcoming the brittleness of glass through bio-inspiration and

micro-architecture," Nat. Commun. 2014 51, vol. 5, no. 1, pp. 1-9, Jan. 2014, doi: 10.1038/ncomms4166.
[55] GCC LaserPro, "C180II User Manual."
[56] Oxford, "Product News," J. Fail. Anal. Prev. 2020 205, vol. 20, no. 5, pp. 1485-1490, Sep. 2020, doi: 10.1007/S11668-020-00992-W.
[57] ASME, Surface Texture (Surface Roughness, Waviness, and Lay) ASME B46.1-2019. USA: ASME, 2019, p. 144.
[58] J. Tullis, C. L. Park, and P. Abbyad, "Selective fusion of anchored droplets via changes in surfactant concentration," Lab Chip, vol. 14, no. 17, pp. 3285-3289, Jul. 2014, doi: 10.1039/C4LC00558A.
[59] H. Y. Lo, Y. Liu, and L. Xu, "Mechanism of contact between a droplet and an atomically smooth substrate," Phys. Rev. X, vol. 7, no. 2, pp. 1-14, 2017, doi: 10.1103/PhysRevX.7.021036.
[60] C. Yan, P. Jiang, X. Jia, and X. Wang, "3D printing of bioinspired textured surfaces with superamphiphobicity," vol. 12, p. 2924, 2020, doi: 10.1039/c9nr09620e.
[61] B. Zhao, C. W. MacMinn, and R. Juanes, "Wettability control on multiphase flow in patterned microfluidics," Proc. Natl. Acad. Sci. U. S. A., vol. 113, no. 37, pp. 10251-10256, Sep. 2016, doi: 10.1073/PNAS.1603387113/SUPPL_FILE/PNAS. 1603387113. SM04. MOV.
[62] B. Steinhaus, P. T. Spicer, and A. Q. Shen, "Droplet Size Effects on Film Drainage between Droplet and Substrate," Langmuir, pp. 5308-5313, 2006, doi: 10.1021/la0531300.
[63] J. Guzowski, P. Korczyk, S. Jakiela, and P. Garstecki, "Device and method for high-throughput, on-demand generation and merging of droplets," Jul. 25, 2012.
[64] S. Lopera and R. D. Mansano, "Plasma-Based Surface Modification of Polydimethylsiloxane for PDMS-PDMS Molding," Int. Sch. Res. Netw. ISRN Polym. Sci., vol. 2012, 2012, doi: 10.5402/2012/767151.
[65] P. Garstecki, M. J. Fuerstman, H. A. Stone, and G. M. Whitesides, "Formation of droplets and bubbles in a microfluidic T-junction-scaling and mechanism of break-up," Lab Chip, vol. 6, no. 3, pp. 437-446, Feb. 2006, doi: 10.1039/B510841A.
[66] 3M, "3M ™ Novec ™ 1700 Electronic Grade Coating," 2000. https://multimedia.3m.com/mws/media/234297O/3m-novec-1720-electronic-grade-coating.pdf.
[67] N. Su et al., "The effect of various sandblasting conditions on surface changes of dental zirconia and shear bond strength between zirconia core and indirect composite resin," J. Adv. Prosthodont., vol. 7, no. 3, pp. 214-223, Jun. 2015, doi: 10.4047/JAP.2015.7.3.214.

## Claims

1. A device for printing ordered arrays of double-emulsion droplets at a substrate under an external aqueous phase comprising a movable printing system comprising a movable stage in Y direction and an application system, and the application system comprises an actuator movable in X-Z directions to which a print head is attached wherein the print head is fluidly connected to the source of a dispersed phase and at least one source of dispersing phase, where the printhead comprises a dispersed phase inlet, at least one dispersant phase inlet, and the inlets are fluidly connected to an outlet channel connected to a chamber for attaching an application needle, **characterised in that** the chamber for attaching the application needle (15) is parallel and coaxial or perpendicular to the outlet channel (7), wherein inner surface of the needle (9) is rendered hydrophobic, preferably fluorophilic, wherein outer surface of the needle (9) is susceptible to wetting by the external aqueous phase, and the movable stage (14) comprises a substrate with a modified surface (10) for dispensing a train of monodisperse double-emulsion droplets, being carrier particles.

2. The device according to claim 1, **characterised in that**, the surface of the substrate (10) is modified by laser ablation, sandblasting or made by coping laser-ablated substrate in polydimethylsiloxane.

3. The device according to claim 1 or 2, **characterised in that**, the substrate (10) is made of glass, polydimethylsiloxane, polytetrafluoroethylene or tetrafluoroethylene-hexafluoropropylene-vinylidenefluoride copolymer.

4. The device according to claim 1 or 2, **characterised in that**, surface of substrate (10) is modified to increase its roughness coefficient when compared to non-modified substrate.

5. The device according to claim 1, **characterised in that**, the dispersed phase inlet channel, at least one dispersant phase inlet channel are connected at right angle.

6. The device according to claim 1, **characterised in that**, height of the inlet channels (7a) and (7b) and of the outlet channel (7) equals their width.

7. The device according to claim 1, **characterised in that**, the substrate is covered with fluoropolymer-based coating.

8. The device according to claim 1, **characterised in that**, it comprises one (17), two (17a, 17b) or three (17a, 17b, 17c) inlets of the dispersed phase, wherein one inlet (17) is fluidly connected with channel (7a) with channel (7b) thus forming T-junction (6), wherein two (17a, 17b) or three (17a, 17b, 17c) inlets are fluidly connected with channels forming Y-junction (6a) from which encompasses channel (7b) fluidly connected with channel (7a) thus forming T-junction (6).

9. A method of printing ordered arrays of double-emulsion droplets on a substrate under an external phase, where suspension of the droplets is generated and applied on a substrate under the external aqueous phase, comprising provision of the device, adjusting and putting into linear motion print head against the substrate, generation of the double-emulsion droplets from at least one dispersed phase and dispersing phase, optionally in the generated droplets cells are incapsulated, and extrusion of the droplets on the substrate, **characterised in that**, the droplets are extruded through a needle (9) with inner diameter $D_{in}$, and diameter of the single droplet D obeys D>w and $D > D_{in}$, where w is height of the inlet channels, where flow rate of the dispersed phase and the dispersing phase is from 3 to 7 μL/min and 10 to 30 μL/min, respectively, preferably the flow rate is constant to generate the droplets of constant diameter, wherein the print head moves with speed of 20 mm/s to 25mm/s versus the substrate, wherein distance d of the needle's tip from the substrate is from $d>D$ to $d<D$, preferably $d=D$, whereas the droplets are generated extruded simultaneously with the translation of the print head, and the external phase comprises surfactant with concentration below critical micelle concentration from 0.001% w/w to 0.1% w/w.

10. The method according to claim 9, **characterised in that**, the double-emulsion comprises inner aqueous phase/-middle phase/external phase, where the inner aqueous phase comprises water, DMEM, minimal essential medium, phosphate-buffered saline or their aqueous solution, the middle phase comprises a fluorinated hydrocarbon, preferably selected from group comprising a solution of Novec 7500 with 2-3% w/w of PFPE-PEG-PFPE fluoro-surfactant, the external phase comprises water, DMEM, minimal essential medium, phosphate-buffered saline or their aqueous solution.

11. The method according to claim 10, **characterised in that**, the surfactant is selected from group comprising: sodium dodecyl sulphate, Pluronic 127, or PFPE-PEG-PFPE fluorosurfactant, preferably sodium dodecyl sulphate or Pluronic 127, wherein the preferable surfactant concentration is 0.1% w/w.

12. The method according to claim 9, **characterised in that**, flow rate ratio of fluorinated phase:inner aqueous phase is from 1:3 to 1:7, preferably 1:7, preferably ordered arrays of the double-emulsion droplets are printed in linear order.

13. The method according to any preceding claim, **characterised in that**, when for generating the double-emulsion droplets at least two dispersed phases are used, the droplets are printed with variable flow rate ratio of the dispersed phases comprising variable concentration of the encapsulated substance, preferably varying in a gradual manner, wherein the total flow rate of the dispersed phases is constant.

14. The method according to claim 9, **characterised in that**, the substrate is modified by laser ablation, sandblasting, made by coping laser-ablated substrate in polydimethylsiloxane or is covered with fluoropolymer-based coating.

15. A use of the device for printing ordered arrays of double-emulsion droplets on a substrate under an external aqueous phase, wherein the droplets may comprise a constant or a varying concentration of an encapsulated substance.

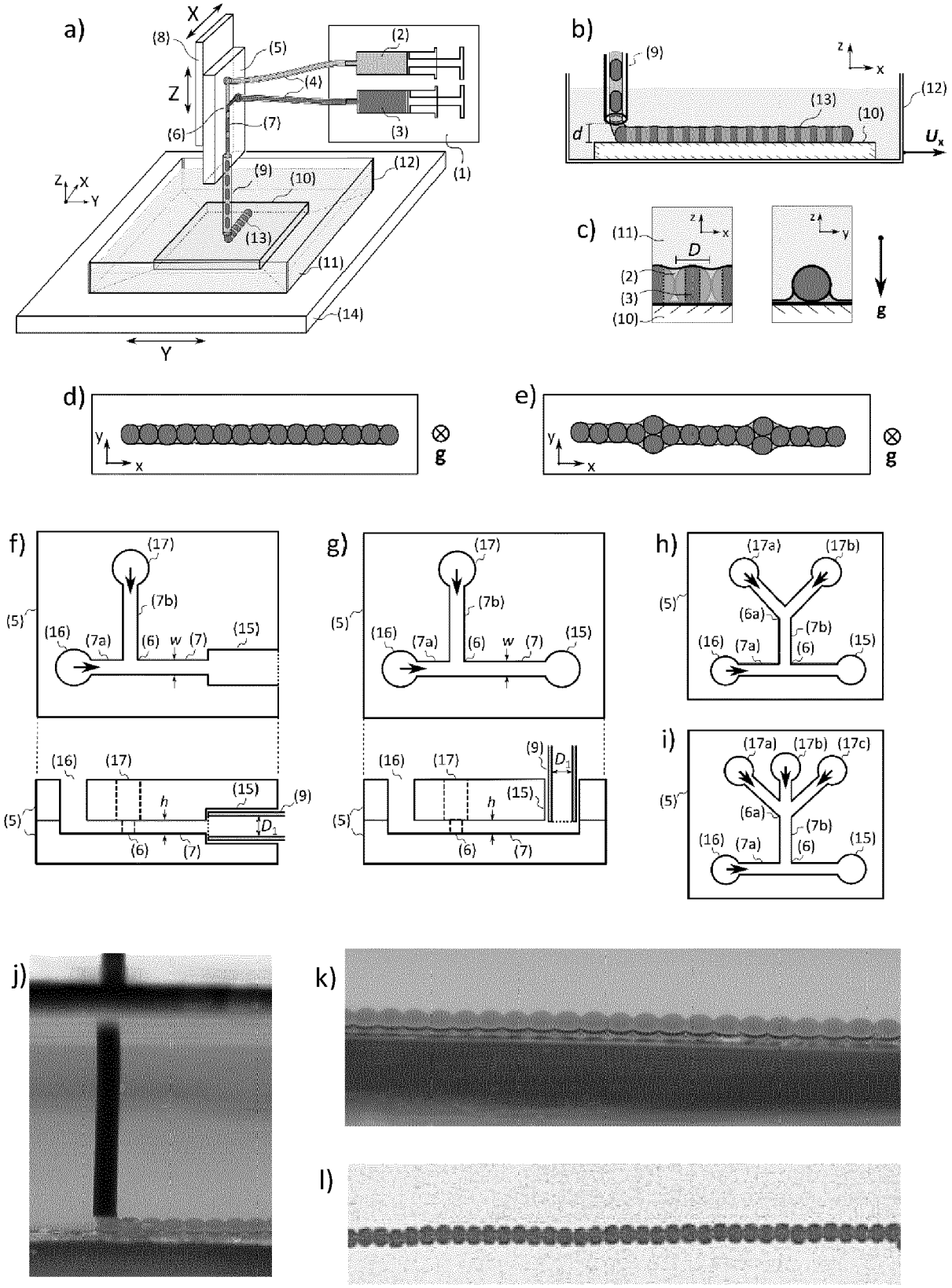
a)
X
Z
Y
(1)
(2)
(3)
(4)
(5)
(6)
(7)
(8)
(9)
(10)
(11)
(12)
(13)
(14)
b)
(9)
(10)
(12)
(13)
d
$U_x$
c)
(11)
D
(2)
(3)
(10)
g
d)
e)
f)
(5)
(6)
(7)
(7a)
(7b)
(15)
(16)
(17)
h
w
(9)
$D_1$
g)
h)
(17a)
(17b)
(6a)
i)
(17c)
j)
k)
l)

Figure 1

a)

| Category | Snapshots — 1 mm |
|---|---|
| Sliding<br>× | 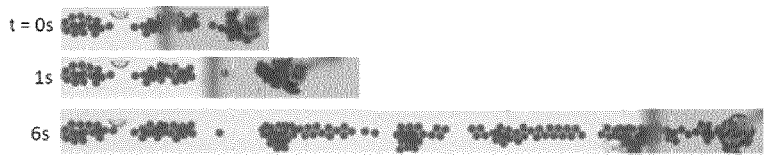 |
| Folding<br>■ | 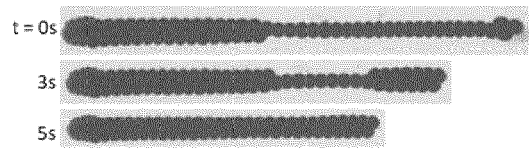 |
| Stable threads<br>(droplets deformed)<br>● | 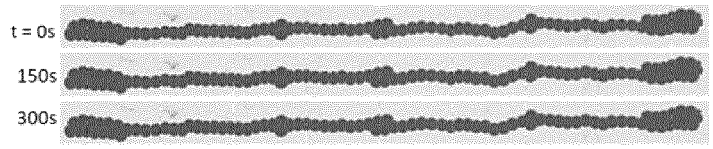 |
| Stable threads<br>○ | 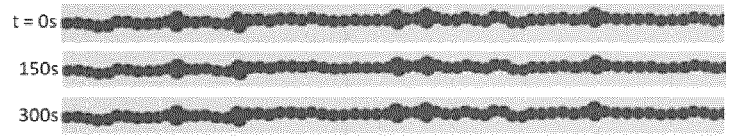 |

b)

**Smooth Substrate ($S_0$)**

| Concentration [% w/w] | 0 | 0,001 | 0,01 | 0,1 | 0,2 | 0,5 | 1,0 |
|---|---|---|---|---|---|---|---|
| SDS | ■ | ■ | ■ | ■ | × | × | × |
| Pluronic F-127 | ■ | ■ | ■ | ■ | ■ | ■ | ■ |

**Rough Substrate ($S_{opt}$)**

| Concentration [% w/w] | 0 | 0,001 | 0,01 | 0,1 | 0,2 | 0,5 | 1,0 |
|---|---|---|---|---|---|---|---|
| SDS | ● | ● | ● | ○ | × | × | × |
| Pluronic F-127 | ● | ● | ● | ● | ● | ● | ● |

**Figure 2 a,b**

c)

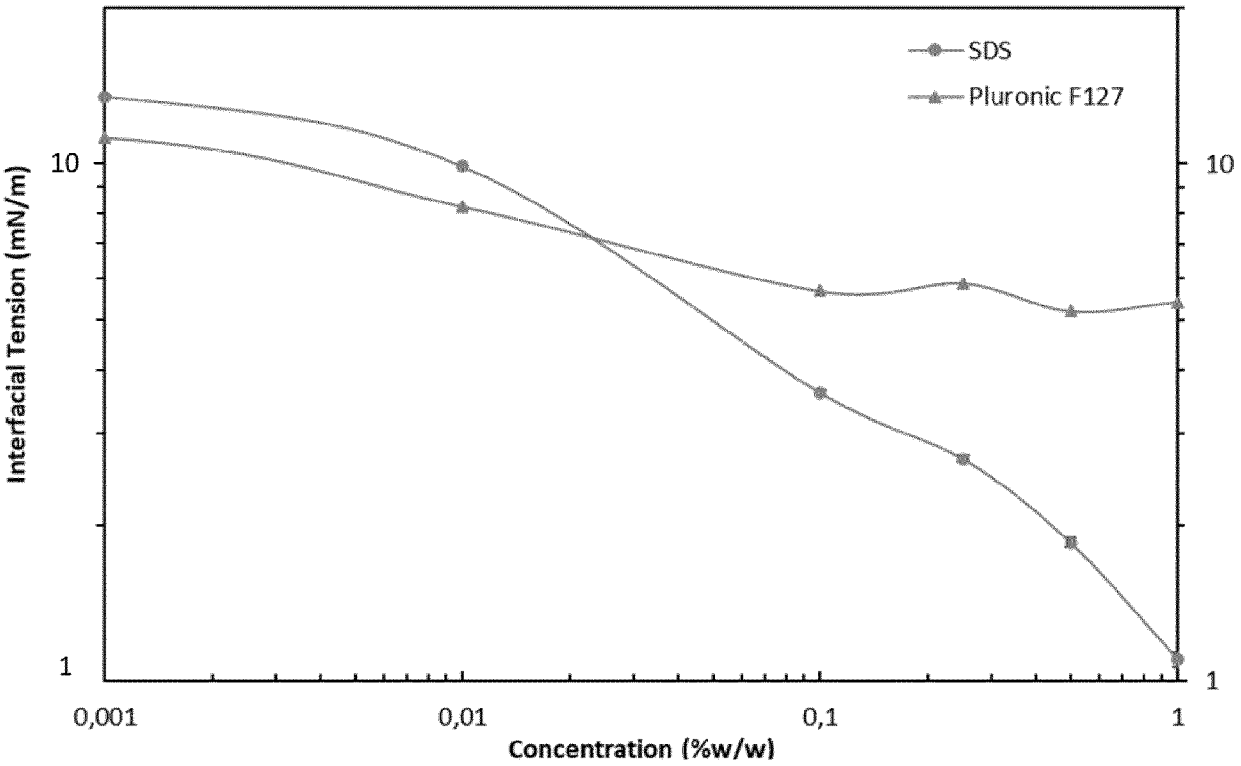
SDS
Pluronic F127
Interfacial Tension (mN/m)
10
1
10
1
0,001
0,01
0,1
1
Concentration (%w/w)

**Figure 2 c**

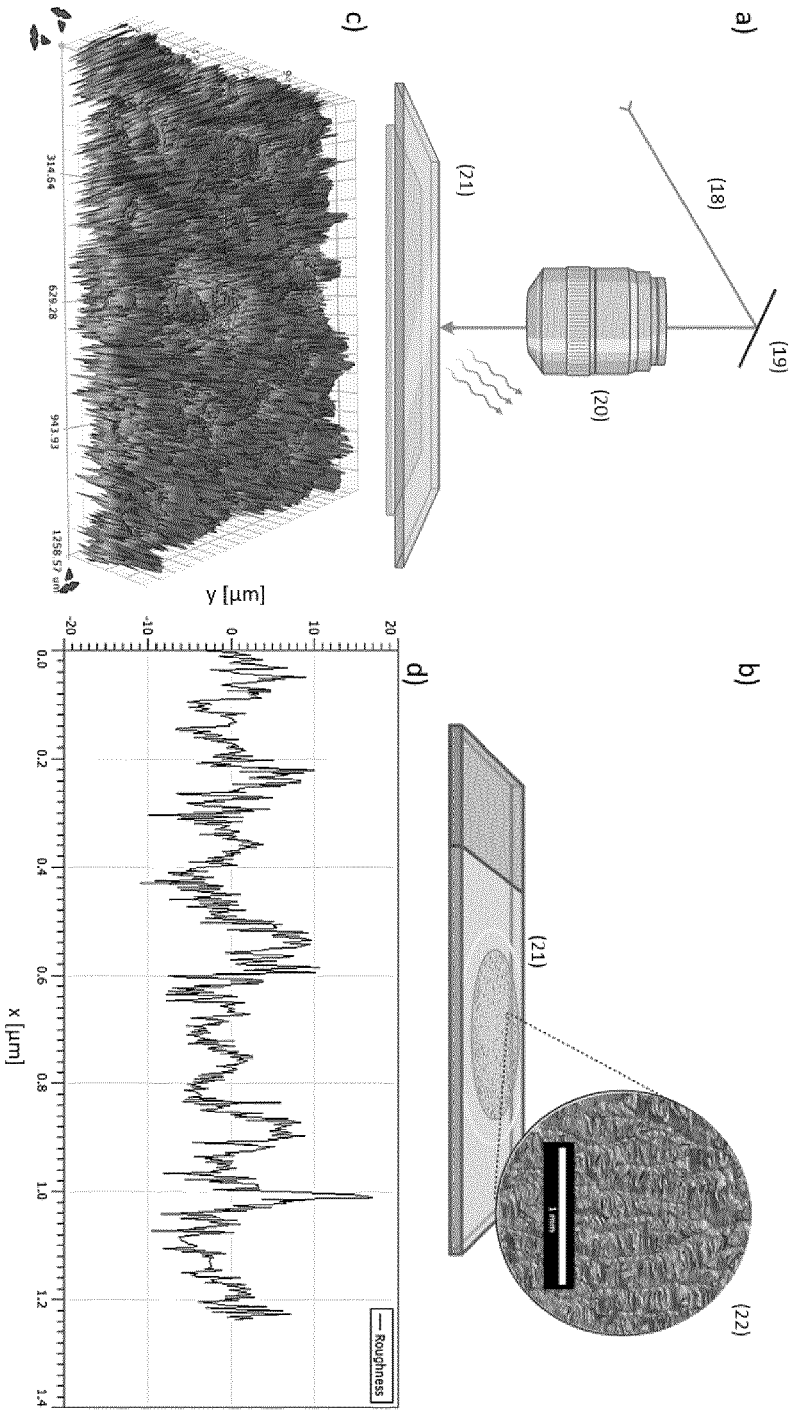


Figure 3

**a)** Droplet spreading at smooth glass ($S_0$).

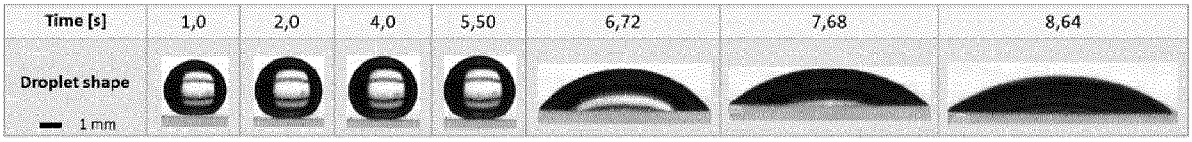


**b)** Droplet spreading at optimally roughened glass ($S_{opt}$).

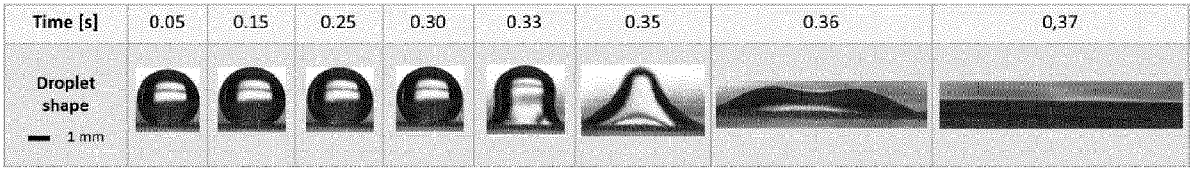


**c)** Drainage time vs. mean squared roughness *R*.

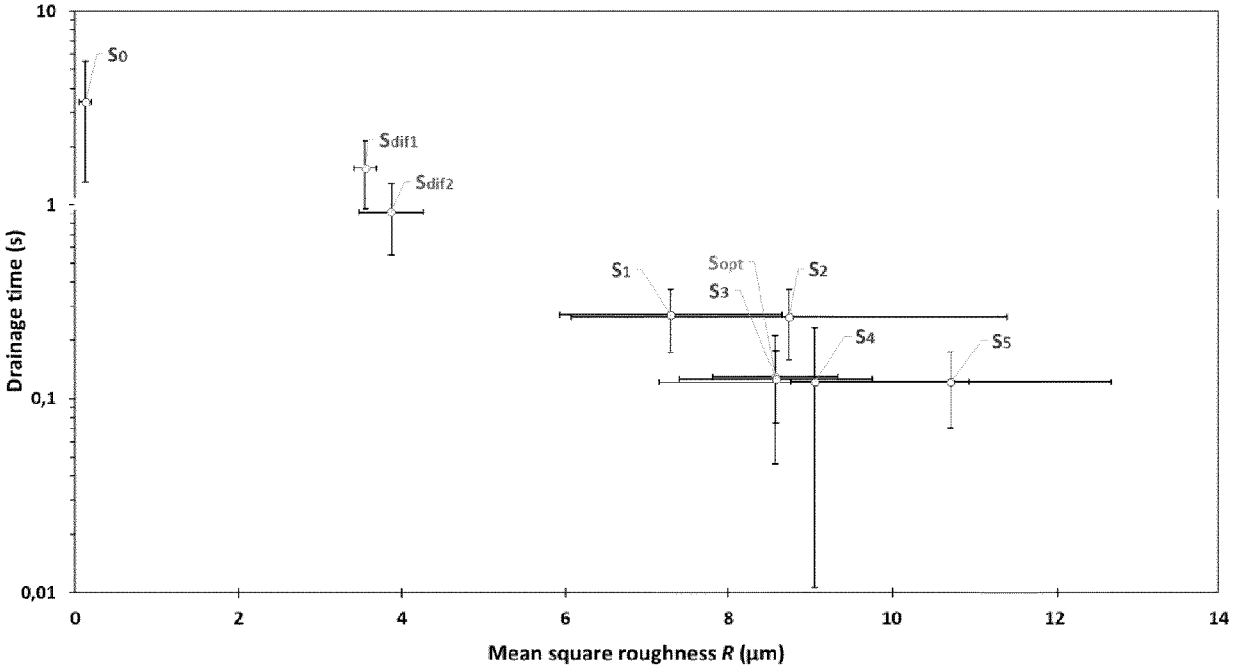


**Figure 4**

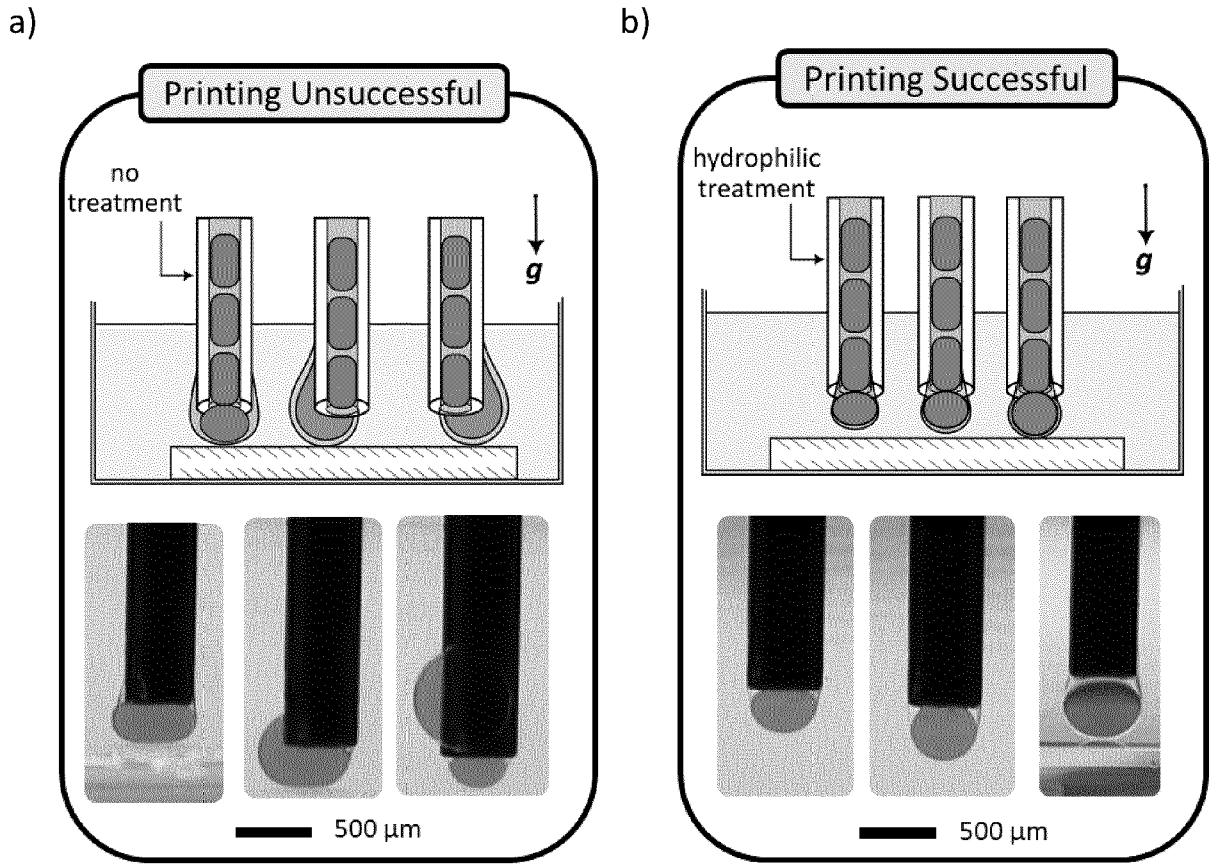
a)
Printing Unsuccessful
no
treatment
g
500 µm
b)
Printing Successful
hydrophilic
treatment
g
500 µm

**Figure 5**

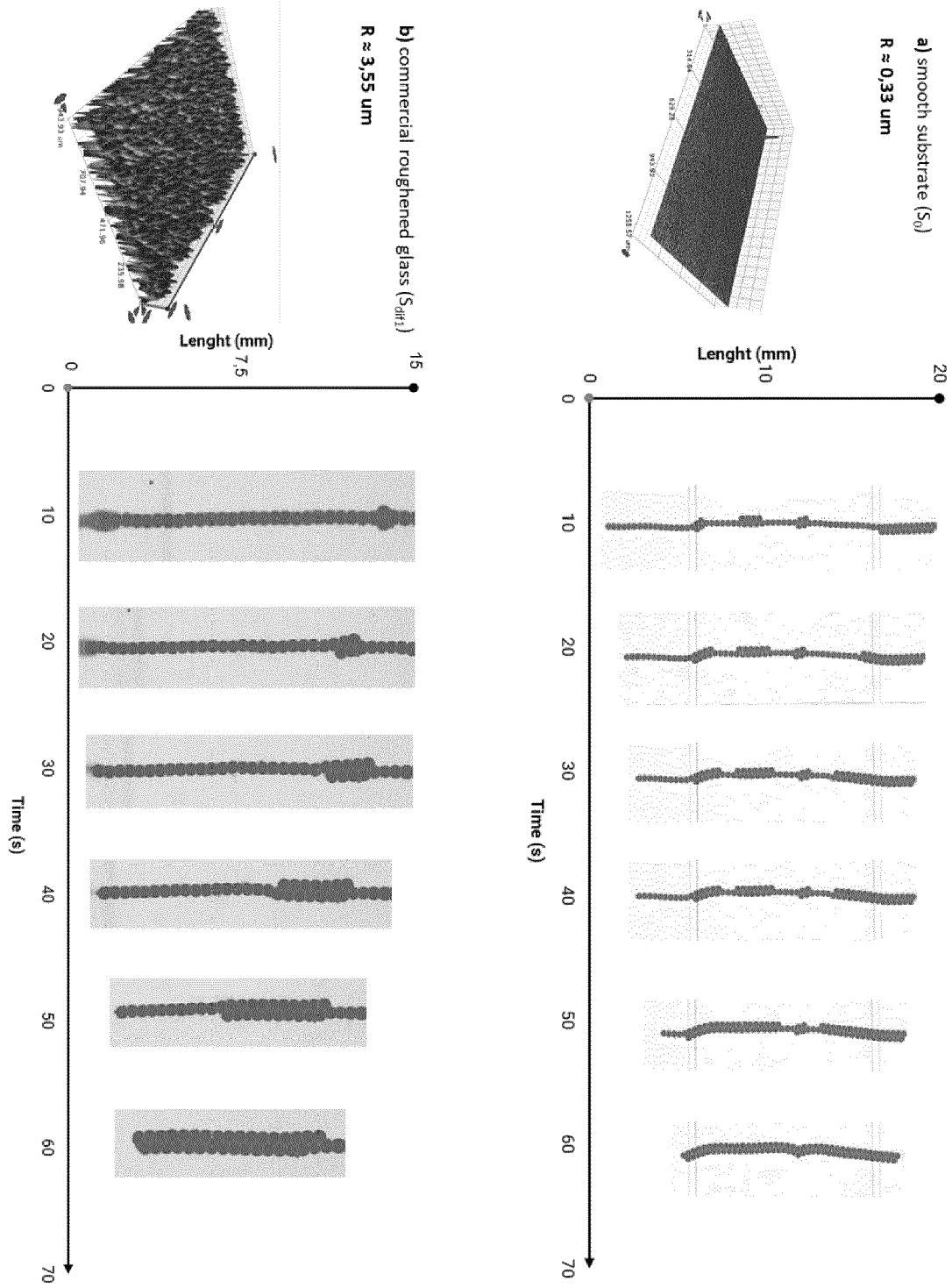
a) smooth substrate ($S_0$)
R ≈ 0,33 um
Lenght (mm)
0
10
20
Time (s)
0
10
20
30
40
50
60
70
b) commercial roughened glass ($S_{diff1}$)
R ≈ 3,55 um
Lenght (mm)
0
7,5
15
Time (s)
0
10
20
30
40
50
60
70

Figure 6

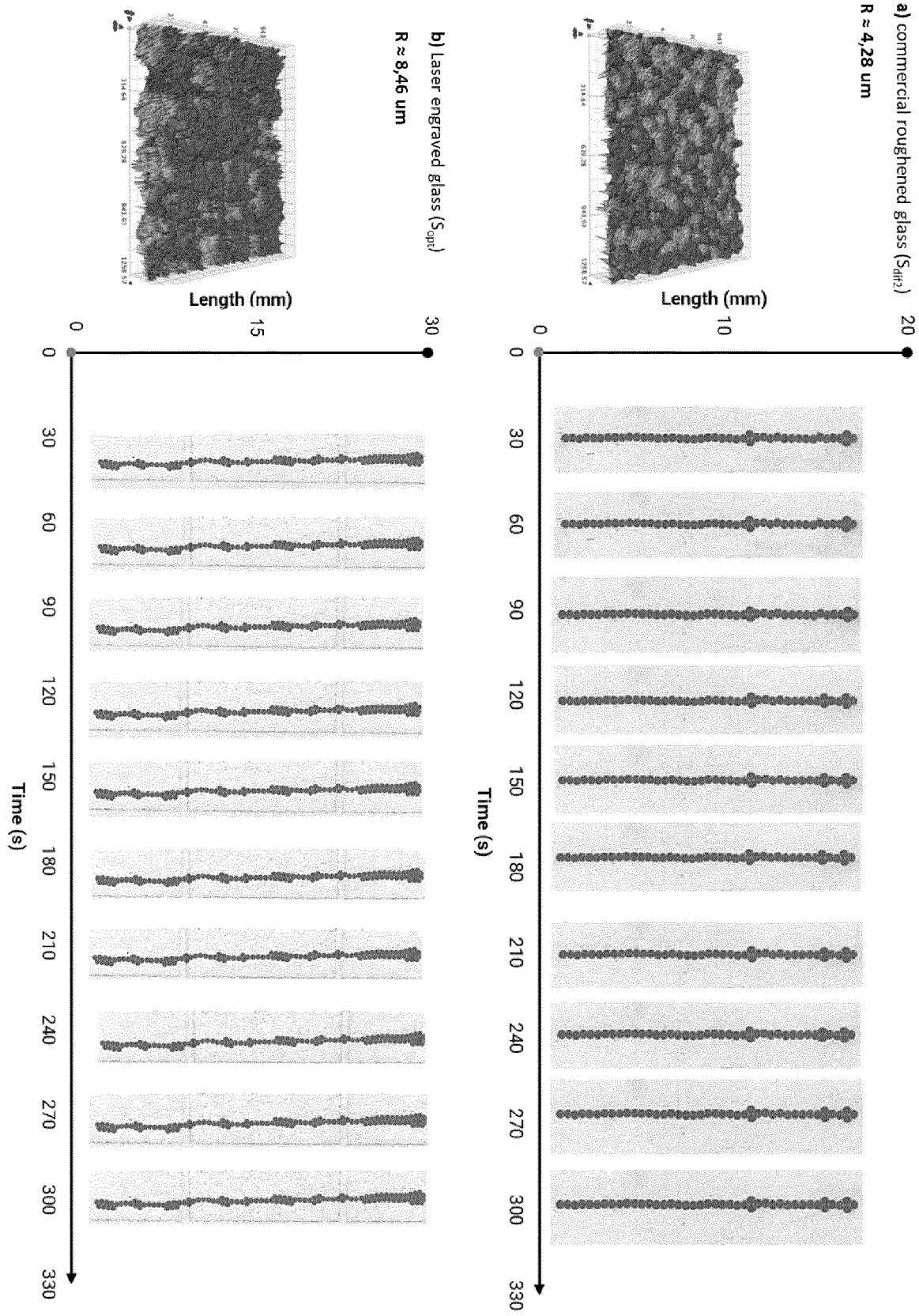
a) commercial roughened glass ($S_{diff2}$)
R ≈ 4,28 um
b) Laser engraved glass ($S_{opt}$)
R ≈ 8,46 um
Length (mm)
Time (s)

Figure 7

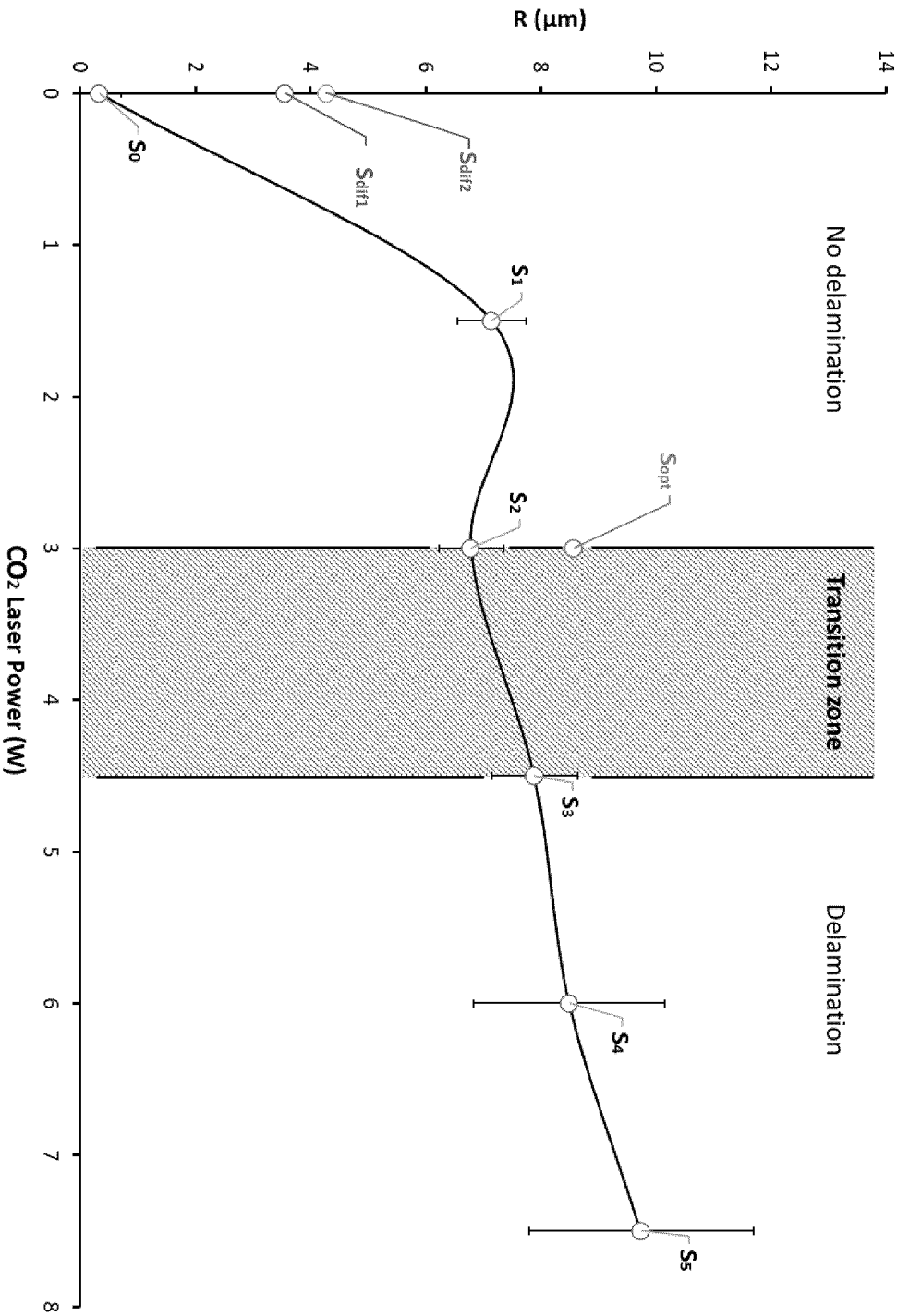
R (µm)
0
2
4
6
8
10
12
14
$S_0$
$S_{dif1}$
$S_{dif2}$
$S_1$
$S_{opt}$
$S_2$
$S_3$
$S_4$
$S_5$
No delamination
Transition zone
Delamination
$CO_2$ Laser Power (W)
0
1
2
3
4
5
6
7
8

Fig. 8

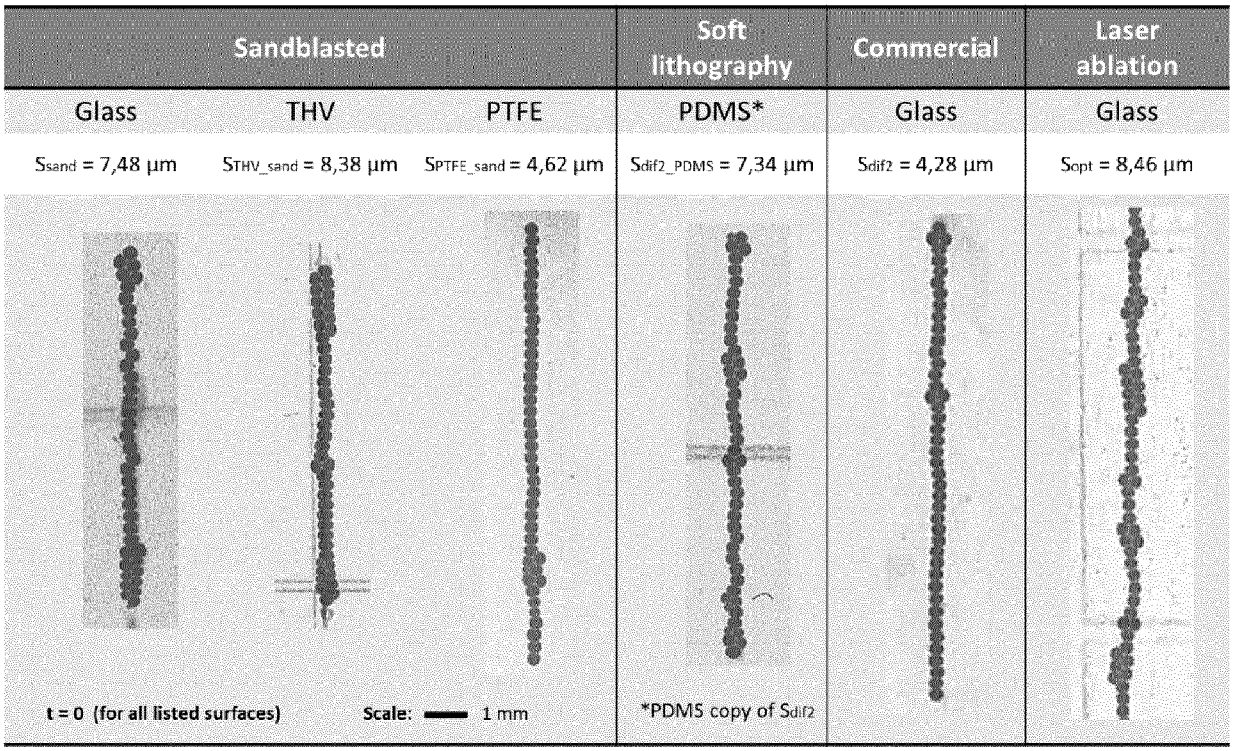
Sandblasted
Soft lithography
Commercial
Laser ablation
Glass
THV
PTFE
PDMS*
Glass
Glass
Ssand = 7,48 µm
STHV_sand = 8,38 µm
SPTFE_sand = 4,62 µm
Sdif2_PDMS = 7,34 µm
Sdif2 = 4,28 µm
Sopt = 8,46 µm
t = 0 (for all listed surfaces)
Scale: 1 mm
*PDMS copy of Sdif2

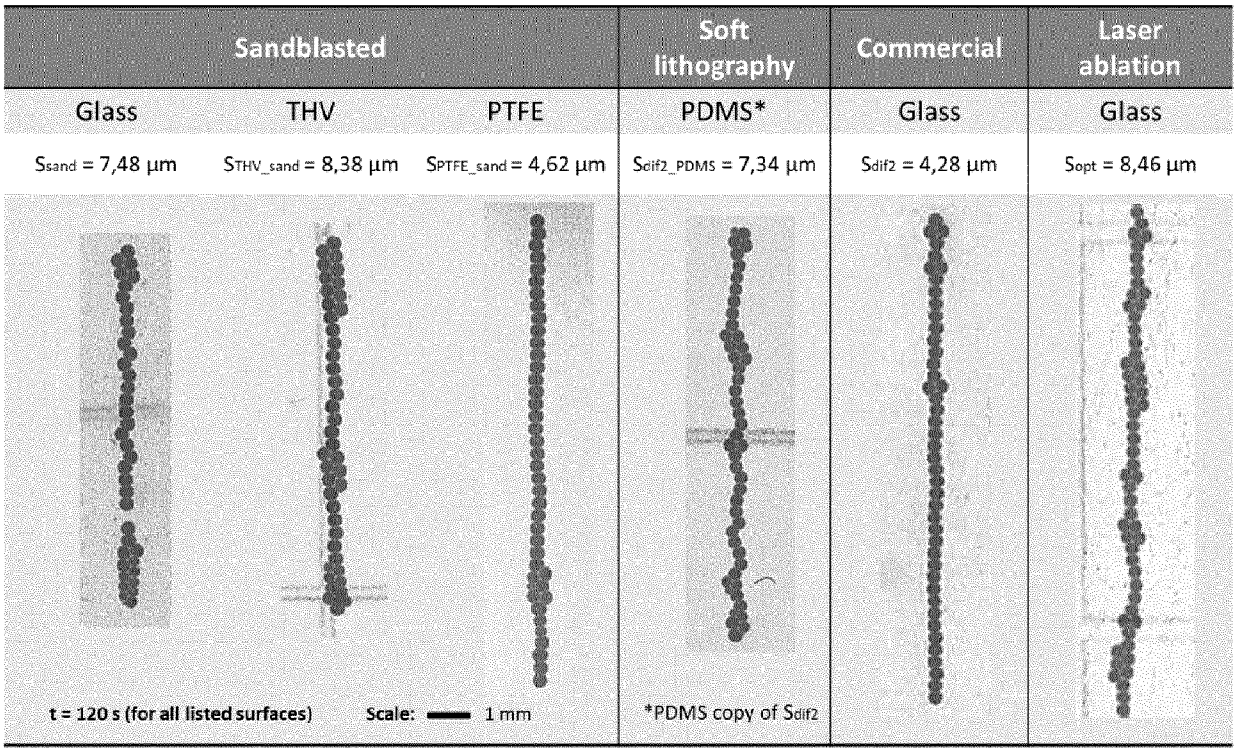
Sandblasted
Soft lithography
Commercial
Laser ablation
Glass
THV
PTFE
PDMS*
Glass
Glass
Ssand = 7,48 µm
STHV_sand = 8,38 µm
SPTFE_sand = 4,62 µm
Sdif2_PDMS = 7,34 µm
Sdif2 = 4,28 µm
Sopt = 8,46 µm
t = 120 s (for all listed surfaces)
Scale: 1 mm
*PDMS copy of Sdif2

**Figure 9**

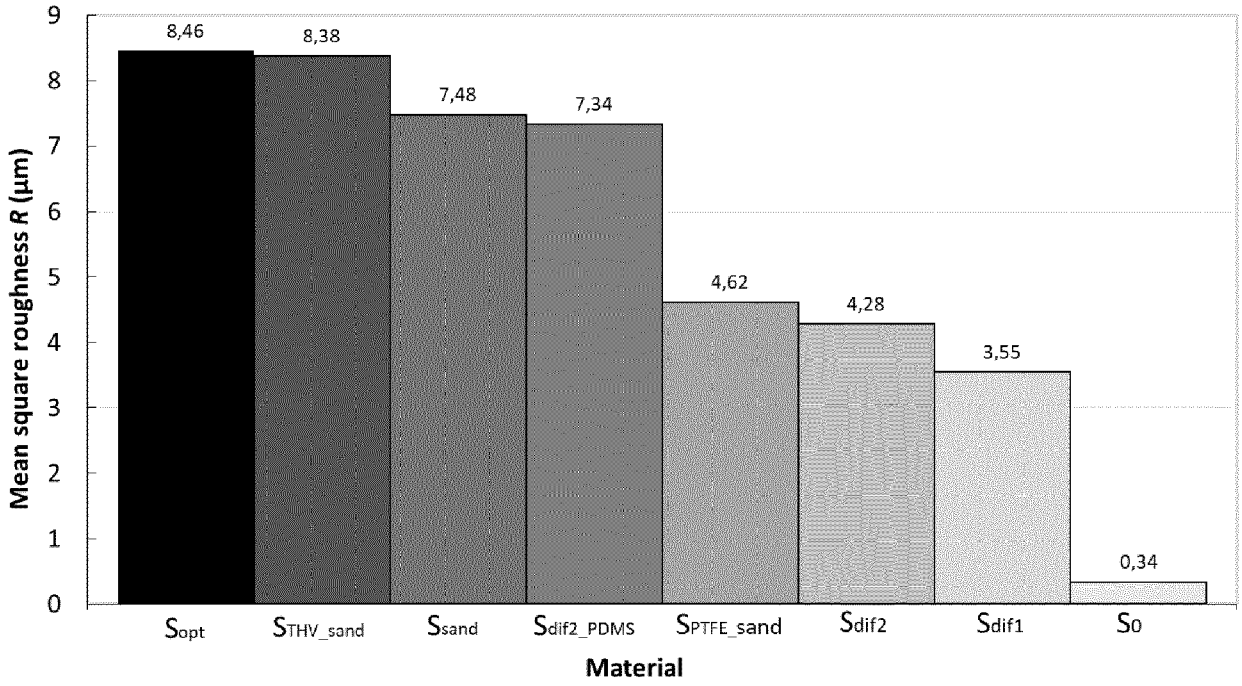
Mean square roughness R (µm)
9
8
7
6
5
4
3
2
1
0
8,46
8,38
7,48
7,34
4,62
4,28
3,55
0,34
Sopt
STHV_sand
Ssand
Sdif2_PDMS
SPTFE_sand
Sdif2
Sdif1
S0
Material

**Figure 10**

**a)** commercial roughened glass ($S_{dif2}$)

**R ≈ 4,28 um**

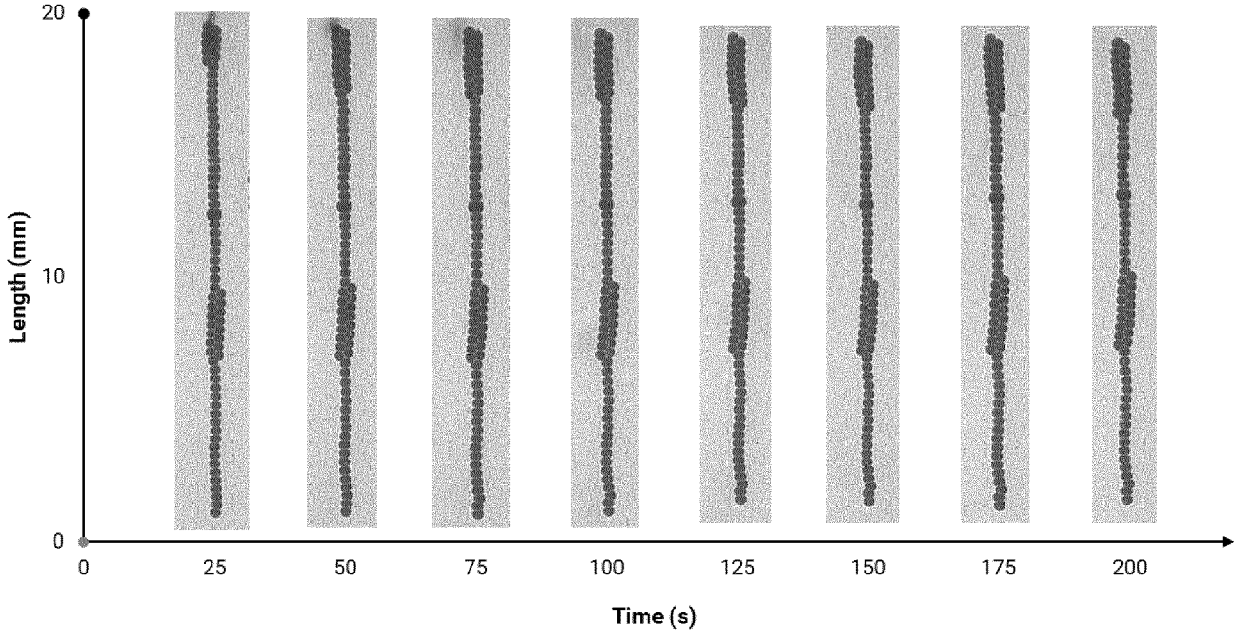


**b)** Laser engraved glass ($S_{opt}$)

**R ≈ 8,46 um**

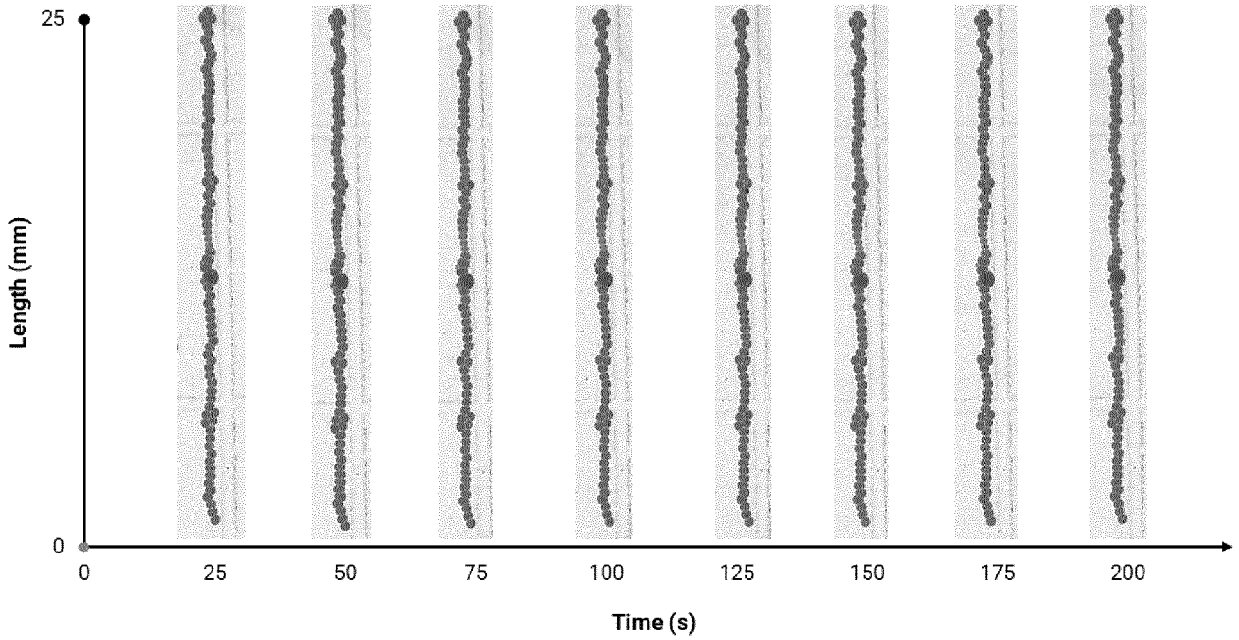


**Figure 11**

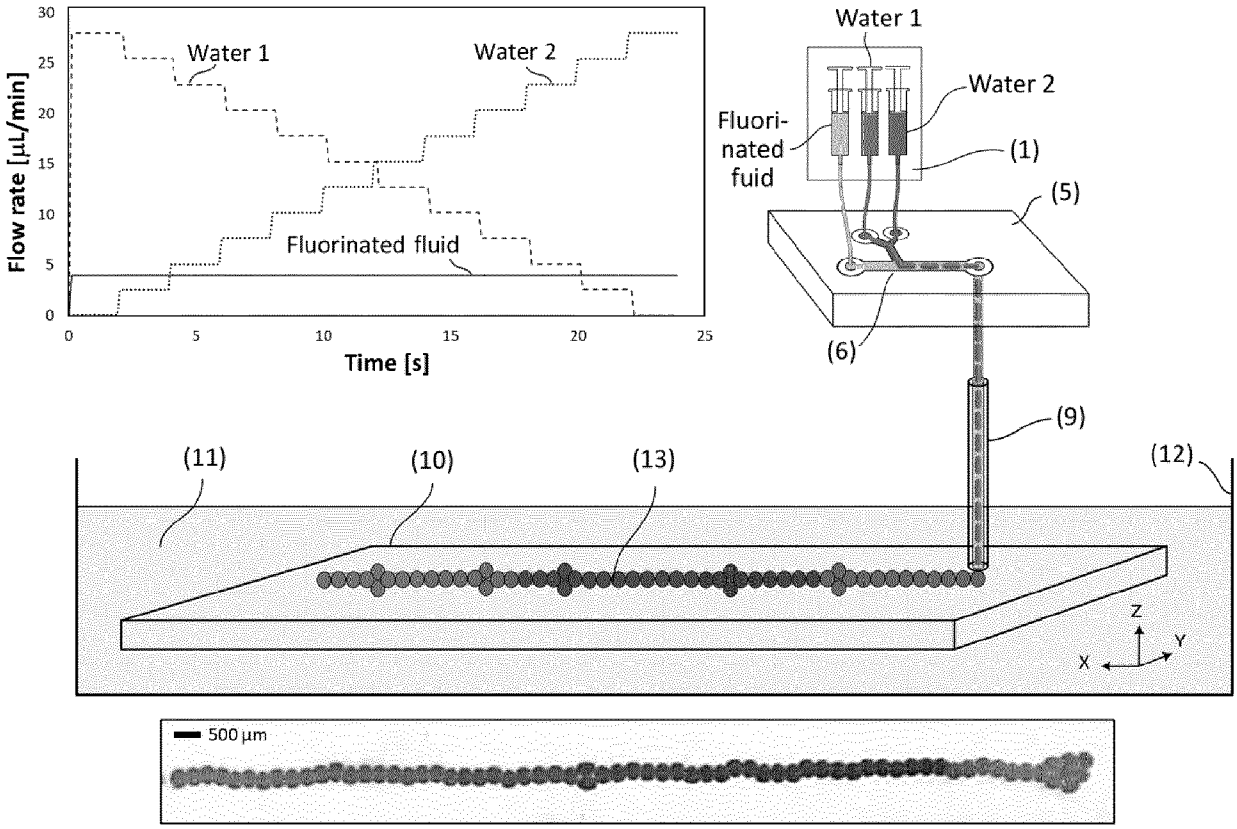


Figure 12

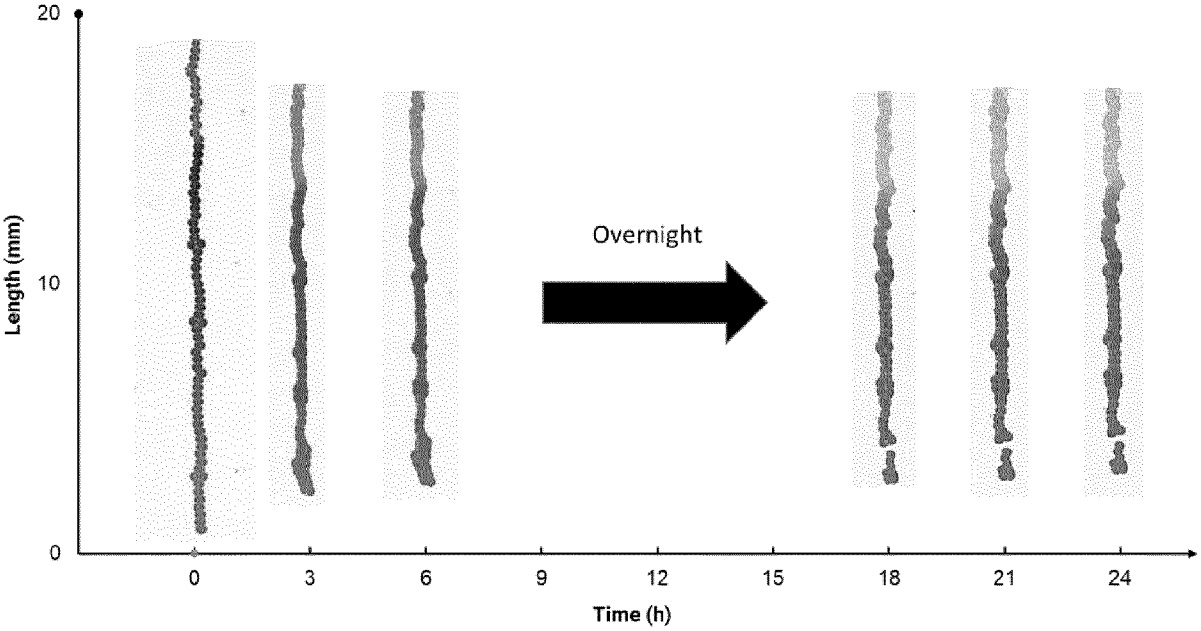


Figure 13

Europäisches Patentamt
European Patent Office
Office européen des brevets

# EUROPEAN SEARCH REPORT

Application Number
EP 23 46 1682

## DOCUMENTS CONSIDERED TO BE RELEVANT

| Category | Citation of document with indication, where appropriate, of relevant passages | Relevant to claim | CLASSIFICATION OF THE APPLICATION (IPC) |
|---|---|---|---|
| X,D | RUSSELL H. COLE ET AL: "Printed droplet microfluidics for on demand dispensing of picoliter droplets and cells", PROCEEDINGS OF THE NATIONAL ACADEMY OF SCIENCES, vol. 114, no. 33, 31 July 2017 (2017-07-31), pages 8728-8733, XP055611136, ISSN: 0027-8424, DOI: 10.1073/pnas.1704020114 * page 8729; figure 1 * | 1-15 | INV. B01L3/00 B01L3/02 |
| A | ROMANOWSKY MARK B. ET AL: "High throughput production of single core double emulsions in a parallelized microfluidic device", LAB ON A CHIP, vol. 12, no. 4, 6 January 2012 (2012-01-06), pages 802-807, XP093050419, UK ISSN: 1473-0197, DOI: 10.1039/c2lc21033a * abstract; figure 1 * | 1-15 | TECHNICAL FIELDS SEARCHED (IPC) B01L |
| A | US 2018/056288 A1 (ABATE ADAM R [US] ET AL) 1 March 2018 (2018-03-01) * the whole document * | 1-15 | |

The present search report has been drawn up for all claims

| Place of search | Date of completion of the search | Examiner |
|---|---|---|
| The Hague | 22 April 2024 | Viskanic, Martino |

CATEGORY OF CITED DOCUMENTS

X : particularly relevant if taken alone
Y : particularly relevant if combined with another document of the same category
A : technological background
O : non-written disclosure
P : intermediate document

T : theory or principle underlying the invention
E : earlier patent document, but published on, or after the filing date
D : document cited in the application
L : document cited for other reasons

& : member of the same patent family, corresponding document

EPO FORM 1503 03.82 (P04C01)

# ANNEX TO THE EUROPEAN SEARCH REPORT ON EUROPEAN PATENT APPLICATION NO. EP 23 46 1682

This annex lists the patent family members relating to the patent documents cited in the above-mentioned European search report. The members are as contained in the European Patent Office EDP file on
The European Patent Office is in no way liable for these particulars which are merely given for the purpose of information.

22-04-2024

| Patent document cited in search report | Publication date | Patent family member(s) | Publication date |
|---|---|---|---|
| US 2018056288 A1 | 01-03-2018 | CA 3001986 A1 | 28-04-2016 |
| | | CN 107107058 A | 29-08-2017 |
| | | EP 3209419 A1 | 30-08-2017 |
| | | US 2018056288 A1 | 01-03-2018 |
| | | US 2020122135 A1 | 23-04-2020 |
| | | WO 2016065056 A1 | 28-04-2016 |

EPO FORM P0459

For more details about this annex : see Official Journal of the European Patent Office, No. 12/82

## REFERENCES CITED IN THE DESCRIPTION

*This list of references cited by the applicant is for the reader's convenience only. It does not form part of the European patent document. Even though great care has been taken in compiling the references, errors or omissions cannot be excluded and the EPO disclaims all liability in this regard.*

### Patent documents cited in the description


- PL P433162 **[0015] [0016] [0029] [0039] [0048] [0072]**
- US 20100022414 A1, M. W. M. Link, Daniel; Hutchison, Brian; Samuel **[0072]**


### Non-patent literature cited in the description


- *CHEMICAL ABSTRACTS*, 297730-93-9 **[0033]**
- *CHEMICAL ABSTRACTS*, 151-21-3 **[0034]**
- *CHEMICAL ABSTRACTS*, 9003-11-6 **[0034]**
- *CHEMICAL ABSTRACTS*, 9016-00-6 **[0046]**
- *CHEMICAL ABSTRACTS*, 9002-84-0 **[0046]**
- *CHEMICAL ABSTRACTS*, 25190-89-0 **[0046]**
- *CHEMICAL ABSTRACTS*, 12660012 **[0050]**
- **Y. DING** ; **P. D. HOWES** ; **J. ANDREW**. *Recent Advances in Droplet Micro fl uidics*, 2020 **[0072]**
- **G. M. WHITESIDES**. The origins and the future of microfluidics. *Nature*, July 2006, vol. 442 (7101), 368-373 **[0072]**
- **M. T. GUO** ; **A. ROTEM** ; **J. A. HEYMAN** ; **D. A. WEITZ**. Droplet microfluidics for high-throughput biological assays. *Lab Chip*, May 2012, vol. 12 (12), 2146-2155 **[0072]**
- **P. ZHU** ; **L. WANG**. Microfluidics-Enabled Soft Manufacture of Materials with Tailorable Wettability. *Chem. Rev.*, April 2022, vol. 122 (7), 7010-7060 **[0072]**
- **A. D. ALADESE** ; **H. H. JEONG**. Recent Developments in 3D Printing of Droplet-Based Microfluidics. *Biochip J.*, December 2021, vol. 15 (4), 313-333 **[0072]**
- **R. CHEN** ; **Z. SUN** ; **D. CHEN**. Droplet-based microfluidics for cell encapsulation and delivery. *Microfluid. Pharm. Appl. From Nano/Micro Syst. Fabr. to Control. Drug Deliv.*, January 2019, 307-335 **[0072]**
- **Y. XING** ; **LOVE LI** ; **XIAOYU YU** ; **E. G. FOX** ; **Y. WANG** ; **J. OBERHOLZER**. Microfuidic Technology for Evaluating and Preserving Islet Function for Islet Transplant in Type 1 Diabetes. *Curr. Transplant. Reports*, August 2022, vol. 1, 10 **[0072]**
- **W. J. SEETO** ; **Y. TIAN** ; **S. PRADHAN** ; **D. MINOND** ; **E. A. LIPKE**. *Droplet Microfluidics-Based Fabrication of Monodisperse Polyethylene glycol)-Fibrinogen Breast Cancer Microspheres for Automated Drug Screening Applications*, 2022 **[0072]**
- **A. PRASTOWO** ; **A. FEUERBORN** ; **P. R. COOK** ; **E. J. WALSH**. Biocompatibility of fluids for multiphase drops-in-drops microfluidics. *Biomed. Microdevices*, 2016, vol. 18 (6), 1-9 **[0072]**
- **A. PRASTOWO** ; **P. R. COOK** ; **E. J. WALSH**. Biocompatibility of Sessile Drops as Chambers for Cell Culture. *Proc. - 2019 2nd Int. Conf. Bioinformatics, Biotechnol. Biomed. Eng. - Bioinforma. Biomed. Eng. BioMIC*, September 2019, vol. 2019 **[0072]**
- **F. QU et al.** Double emulsion-pretreated microwell culture for the in vitro production of multicellular spheroids and their in situ analysis. *Microsystems Nanoeng.*, May 2021, vol. 7 (1), 1-12 **[0072]**
- **A. KUMAR** ; **R. KAUR** ; **V. KUMAR** ; **S. KUMAR** ; **R. GEHLOT** ; **P. AGGARWAL**. New insights into water-in-oil-in-water (W/O/W) double emulsions: Properties, fabrication, instability mechanism, and food applications. *Trends Food Sci. Technol.*, October 2022, vol. 128, 22-37 **[0072]**
- **H. GUDAPATI** ; **M. DEY** ; **I. OZBOLAT**. A comprehensive review on droplet-based bioprinting: Past, present and future. *Biomaterials*, 2016, vol. 102, 20-42 **[0072]**
- **J. K. NUNES** ; **S. S. H. TSAI** ; **J. WAN** ; **H. A. STONE**. Dripping and jetting in microfluidic multiphase flows applied to particle and fibre synthesis. *J. Phys. D. Appl. Phys.*, March 2013, vol. 46 (11) **[0072]**
- **P. GARSTECKI** ; **M. J. FUERSTMAN** ; **A. STONE** ; **G. M. WHITESIDES**. *Formation of droplets and bubbles in a microfluidic T-junction - scaling and mechanism of break-up*, 2006, 437-446 **[0072]**
- **J. GUZOWSKI** ; **S. JAKIELA** ; **P. M. KORCZYK BC** ; **P. GARSTECKI**. Custom tailoring multiple droplets one-by-one + Lab on a Chip. *Pol. Akad. Nauk Inst. Chem. Fiz.*, 2013, vol. 13, 4308-4311 **[0072]**
- **F. M. GALOGAHI** ; **Y. ZHU** ; **H. AN** ; **N.-T. NGUYEN**. *Formation of core-shell droplets for the encapsulation of liquid contents*, 2021, vol. 25, 82 **[0072]**
- **F. M. GALOGAHI** ; **Y. ZHU** ; **H. AN** ; **N. T. NGUYEN**. Core-shell microparticles: Generation approaches and applications. *J. Sci. Adv. Mater. Devices*, December 2020, vol. 5 (4), 417-435 **[0072]**
- **K. K. BROWER et al.** Double emulsion flow cytometry with high-throughput single droplet isolation and nucleic acid recovery. *Lab Chip*, June 2020, vol. 20 (12), 2062-2074 **[0072]**

- **K. K. BROWER et al.** Double Emulsion Picoreactors for High-Throughput Single-Cell Encapsulation and Phenotyping via FACS. *Anal. Chem.*, October 2020, vol. 92 (19), 13262-13270 **[0072]**
- **W. JIANG** ; **M. LI** ; **Z. CHEN** ; **K. W. LEONG**. Cell-laden microfluidic microgels for tissue regeneration. *Lab Chip*, November 2016, vol. 16 (23), 4482-4506 **[0072]**
- **H. F. CHAN** ; **Y. ZHANG** ; **Y. P. HO** ; **Y. L. CHIU** ; **Y. JUNG** ; **K. W. LEONG**. Rapid formation of multicellular spheroids in double-emulsion droplets with controllable microenvironment. *Sci. Reports*, 31 December 2013, vol. 3 (1), 1-8 **[0072]**
- **S. C. RAMAIAHGARI et al.** A 3D in vitro model of differentiated HepG2 cell spheroids with improved liver-like properties for repeated dose high-throughput toxicity studies. *Arch. Toxicol.*, March 2014, vol. 88 (5), 1083-1095 **[0072]**
- **T. A. DUNCOMBE** ; **P. S. DITTRICH**. Droplet barcoding: tracking mobile micro-reactors for high-throughput biology. *Curr. Opin. Biotechnol.*, December 2019, vol. 60, 205-212 **[0072]**
- **E. BROUZES et al.** *Droplet microfluidic technology for single-cell high-throughput screening*, 2009 **[0072]**
- **R. F. X. TOMASI** ; **S. SART** ; **T. CHAMPETIER** ; **C. N. BAROUD**. Individual Control and Quantification of 3D Spheroids in a High-Density Microfluidic Droplet Array. *Cell Rep.*, May 2020, vol. 31 (8), 107670 **[0072]**
- **J. Q. BOEDICKER** ; **L. LI** ; **T. R. KLINE** ; **R. F. ISMAGILOV**. Detecting bacteria and determining their susceptibility to antibiotics by stochastic confinement in nanoliter droplets using plug-based microfluidics. *Lab Chip*, July 2008, vol. 8 (8), 1265-1272 **[0072]**
- **K. CHURSKI et al.** Rapid screening of antibiotic toxicity in an automated microdroplet system. *Lab Chip*, April 2012, vol. 12 (9), 1629-1637 **[0072]**
- **F. EDUATI et al.** A microfluidics platform for combinatorial drug screening on cancer biopsies. *Nat. Commun.*, June 2018, vol. 9 (1), 1-13 **[0072]**
- **R. H. COLE et al.** Printed droplet microfluidics for on demand dispensing of picoliter droplets and cells. *Proc. Natl. Acad. Sci. U. S. A.*, 2017, vol. 114 (33), 8728-8733 **[0072]**
- **S. SAKAKIHARA** ; **S. ARAKI** ; **R. LINO** ; **H. NOJI**. A single-molecule enzymatic assay in a directly accessible femtoliter droplet array. *Lab Chip,*, December 2010, vol. 10 (24), 3355-3362 **[0072]**
- **S. K. KÜSTER et al.** Interfacing droplet microfluidics with matrix-assisted laser desorption/ionization mass spectrometry: Label-free content analysis of single droplets. *Anal. Chem.*, February 2013, vol. 85 (3), 1285-1289 **[0072]**
- **Y. BAI** ; **E. WEIBULL** ; **H. N. JOENSSON** ; **H. ANDERSSON-SVAHN**. Interfacing picoliter droplet microfluidics with addressable microliter compartments using fluorescence activated cell sorting. *Sensors Actuators B Chem.*, April 2014, vol. 194, 249-254 **[0072]**
- **S. SART** ; **R. TOMASI** ; **G. AMSELEM** ; **C. N. BAROUD**. Multiscale cytometry and regulation of 3D cell cultures on a chip. *Nat. Commun.*, 2017, vol. 8 (1), 469 **[0072]**
- **D. HAIDAS** ; **M. NAPIORKOWSKA** ; **S. SCHMITT** ; **P. S. DITTRICH**. Parallel Sampling of Nanoliter Droplet Arrays for Noninvasive Protein Analysis in Discrete Yeast Cultivations by MALDI-MS. *Anal. Chem.*, March 2020, vol. 92 (5), 3810-3818 **[0072]**
- **X. LI** ; **J. M. ZHANG** ; **X. YI** ; **Z. HUANG** ; **P. LV** ; **H. DUAN**. Multimaterial Microfluidic 3D Printing of Textured Composites with Liquid Inclusions. *Adv. Sci.*, 2019, vol. 6 (3), 1-7 **[0072]**
- **A. Z. NELSON** ; **B. KUNDUKAD** ; **W. K. WONG** ; **S. A. KHAN** ; **P. S. DOYLE**. Embedded droplet printing in yield-stress fluids. *Proc. Natl. Acad. Sci. U. S. A.*, March 2020, vol. 117 (11), 5671-5679 **[0072]**
- **S. MA**. Microfluidics tubing as a synthesizer for ordered microgel networks Microfluidics tubing as a synthesizer for ordered microgel networks. *Soft Matter*, 2019, vol. 15 (19), 3848 **[0072]**
- **L. ZHOU et al.** Lipid-Bilayer-Supported 3D Printing of Human Cerebral Cortex Cells Reveals Developmental Interactions. *Adv. Mater.*, August 2020, vol. 32 (31), 2002183 **[0072]**
- **A. ALCINESIO et al.** Controlled packing and single-droplet resolution of 3D-printed functional synthetic tissues. *Nat. Commun.*, 2020, vol. 11 (1), 2105 **[0072]**
- **Y. K. LAI** ; **A. S. OPALSKI** ; **P. GARSTECKI** ; **L. DERZSI** ; **J. GUZOWSKI**. A double-step emulsification device for direct generation of double emulsions. *Soft Matter*, August 2022, vol. 18 (33), 6157-6166 **[0072]**
- **L. AMIRIFAR et al.** Droplet-based microfluidics in biomedical applications. *Biofabrication*, January 2022, vol. 14 (2), 022001 **[0072]**
- **S. M. GIANNITELLI et al.** Droplet-based microfluidic synthesis of nanogels for controlled drug delivery: tailoring nanomaterial properties via pneumatically actuated flow-focusing junction. *Nanoscale*, August 2022, vol. 14 (31), 11415-11428 **[0072]**
- **C. LI et al.** Under-Oil Autonomously Regulated Oxygen Microenvironments: A Goldilocks Principle-Based Approach for Microscale Cell Culture. *Adv. Sci.*, April 2022, vol. 9 (10) **[0072]**
- **C. HOLTZE et al.** Biocompatible surfactants for water-in-fluorocarbon emulsions. *Lab Chip*, 2008, vol. 8 (10), 1632 **[0072]**
- **J.-C. BARET**. Surfactants in droplet-based microfluidics †. *Lab Chip*, February 2012, vol. 12 (3), 403-664 **[0072]**

- **G. AUBRY** ; **M. ZHAN** ; **H. LU**. Hydrogel-droplet microfluidic platform for high-resolution imaging and sorting of early larval Caenorhabditis elegans. *Lab Chip*, March 2015, vol. 15 (6), 1424 **[0072]**
- **M. LI et al.** A versatile platform for surface modification of microfluidic droplets. *Lab Chip*, February 2017, vol. 17 (4), 635 **[0072]**
- **B. HAMMOUDA**. Temperature Effect on the Nanostructure of SDS Micelles in Water. *J. Res. Natl. Inst. Stand. Technol.*, 2013, vol. 118, 151-167 **[0072]**
- **Q. GAO** ; **Q. LIANG** ; **F. YU** ; **J. XU** ; **Q. ZHAO** ; **B. SUN**. Synthesis and characterization of novel amphiphilic copolymer stearic acid-coupled F127 nanoparticles for nano-technology based drug delivery system. *Colloids Surfaces B Biointerfaces*, 2011, vol. 88, 741-748 **[0072]**
- **M. MIRKHALAF** ; **A. K. DASTJERDI** ; **F. BARTHELAT**. Overcoming the brittleness of glass through bio-inspiration and micro-architecture. *Nat. Commun.*, January 2014, vol. 5 (1), 1-9 **[0072]**
- Product News. *J. Fail. Anal. Prev.*, September 2020, vol. 20 (5), 1485-1490 **[0072]**
- Surface Texture (Surface Roughness, Waviness, and Lay) ASME B46.1-2019. ASME, 2019, 144 **[0072]**
- **J. TULLIS** ; **C. L. PARK** ; **P. ABBYAD**. Selective fusion of anchored droplets via changes in surfactant concentration. *Lab Chip*, July 2014, vol. 14 (17), 3285-3289 **[0072]**
- **H. Y. LO** ; **Y. LIU** ; **L. XU**. Mechanism of contact between a droplet and an atomically smooth substrate. *Phys. Rev. X*, 2017, vol. 7 (2), 1-14 **[0072]**
- **C. YAN** ; **P. JIANG** ; **X. JIA** ; **X. WANG**. *3D printing of bioinspired textured surfaces with superamphiphobicity*, 2020, vol. 12, 2924 **[0072]**
- **B. ZHAO** ; **C. W. MACMINN** ; **R. JUANES**. Wettability control on multiphase flow in patterned microfluidics. *Proc. Natl. Acad. Sci. U. S. A.*, September 2016, vol. 113 (37), 10251-10256 **[0072]**
- **B. STEINHAUS** ; **P. T. SPICER** ; **A. Q. SHEN**. Droplet Size Effects on Film Drainage between Droplet and Substrate. *Langmuir*, 2006, 5308-5313 **[0072]**
- **J. GUZOWSKI** ; **P. KORCZYK** ; **S. JAKIELA** ; **P. GARSTECKI**. *Device and method for high-throughput, on-demand generation and merging of droplets*, 25 July 2012 **[0072]**
- **S. LOPERA** ; **R. D. MANSANO**. Plasma-Based Surface Modification of Polydimethylsiloxane for PDMS-PDMS Molding. *Int. Sch. Res. Netw. ISRN Polym. Sci.*, 2012, vol. 2012 **[0072]**
- **P. GARSTECKI** ; **M. J. FUERSTMAN** ; **H. A. STONE** ; **G. M. WHITESIDES**. Formation of droplets and bubbles in a microfluidic T-junction-scaling and mechanism of break-up. *Lab Chip*, February 2006, vol. 6 (3), 437-446 **[0072]**
- *3M, "3M Novec 1700 Electronic Grade Coating*, 2000 **[0072]**
- **N. SU et al.** The effect of various sandblasting conditions on surface changes of dental zirconia and shear bond strength between zirconia core and indirect composite resin. *J. Adv. Prosthodont.*, June 2015, vol. 7 (3), 214-223 **[0072]**